AD-A088 735 TEXAS UNIV AT EL PASO SCHELLENGER RESEARCH LABS F/G 4/1
GERDIEN CONDENSER INSTRUMENTATION FOR MEASURING HIGH-LATITUDE M--ETC(U)
MAY 79 K DOMAGALSKI, J D MITCHELL DAAD07-78-C-0010
UNCLASSIFIED SR2-80-UA-76 NL

1 OF 1
AD
A088735

END
DATE
FILMED
10-80
DTIC

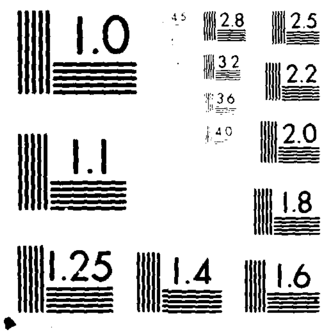

MICROCOPY RESOLUTION TEST CHART

NATIONAL BUREAU OF STANDARDS 1963-A

LEVEL II

1

SCHELLENGER RESEARCH LABORATORIES

ELECTRICAL ENGINEERING DEPARTMENT

GERDIEN CONDENSER INSTRUMENTATION FOR MEASURING
HIGH-LATITUDE MIDDLE ATMOSPHERE ELECTRICAL PARAMETERS

AD A088735

ENGINEERING AND SCIENCE COMPLEX

The University of Texas
at El Paso

80 6 23 016

GERDIEN CONDENSER INSTRUMENTATION FOR MEASURING HIGH-LATITUDE MIDDLE ATMOSPHERE ELECTRICAL PARAMETERS.

SPECIAL REPORT. 5/31/79 SR2-80-UA-76

Prepared For:

United States Army Electronics Command
Atmospheric Sciences Laboratory
White Sands Missile Range
New Mexico

31 May 79

79

Submitted By:

Electrical Engineering Department
The University of Texas at El Paso
El Paso, Texas

DAAD07-78-C-0012

Klaus Domagalski
Graduate Research Assistant

John D. Mitchell
Associate Professor

388763

SECURITY CLASSIFICATION OF THIS PAGE (When Data Entered)

REPORT DOCUMENTATION PAGE		READ INSTRUCTIONS BEFORE COMPLETING FORM
1. REPORT NUMBER SR2-80-UA-76	2. GOVT ACCESSION NO. AD-088 735	3. RECIPIENT'S CATALOG NUMBER
4. TITLE (and Subtitle) ~~Upper Atmospheric Research~~ "Gerdien Condenser Instrumentation for Measuring High-Latitude Middle Atmosphere Electrical Parameters"		5. TYPE OF REPORT & PERIOD COVERED Special Report May 1979
		6. PERFORMING ORG. REPORT NUMBER
7. AUTHOR(s) Klaus Domagalski and John D. Mitchell		8. CONTRACT OR GRANT NUMBER(s) DAAD07-78-C-0010
9. PERFORMING ORGANIZATION NAME AND ADDRESS Schellenger Research/Electrical Engr. Dept The University of Texas at El Paso El Paso, Texas 79968		10. PROGRAM ELEMENT, PROJECT, TASK AREA & WORK UNIT NUMBERS
11. CONTROLLING OFFICE NAME AND ADDRESS		12. REPORT DATE May 1979
		13. NUMBER OF PAGES 68
14. MONITORING AGENCY NAME & ADDRESS(if different from Controlling Office)		15. SECURITY CLASS. (of this report) Unclassified
		15a. DECLASSIFICATION/DOWNGRADING SCHEDULE

16. DISTRIBUTION STATEMENT (of this Report)

DISTRIBUTION STATEMENT A
Approved for public release;
Distribution Unlimited

17. DISTRIBUTION STATEMENT (of the abstract entered in Block 20, if different from Report)

Approved for public release. Distribution unlimited.

18. SUPPLEMENTARY NOTES

Contract Monitor: Mr. Robert Rubio
Atmospheric Science Laboratory
White Sands Missile Range
New Mexico 88002

19. KEY WORDS (Continue on reverse side if necessary and identify by block number)

Middle atmosphere, ionization, Gerdien condenser, electrical conductivity, rocket instrumentation

20. ABSTRACT (Continue on reverse side if necessary and identify by block number)

Gerdien condensers for measuring electrical conductivity, ion mobility and charge number density were flown in recent rocket programs to investigate the high-latitude middle atmosphere. The instruments were launched in two coordinated programs (Aurorozone I and II) at Poker Flat, Alaska to study the effects of auroral energetics on electrical parameters and in a solar eclipse rocket program at Red Lake, Canada. The design of the

DD FORM 1 JAN 73 1473 EDITION OF 1 NOV 65 IS OBSOLETE

SECURITY CLASSIFICATION OF THIS PAGE (When Data Entered)

Gerdien condenser instrumentation for the Aurorozone II program and the solar eclipse program is considered. In addition, electrical parameters measured for the two auroral programs are presented and discussed. The initial results from the measurements indicate that high-latitude middle atmosphere electrical parameters are strongly influenced by the auroral energetics.

ABSTRACT

Gerdien condensers for measuring electrical conductivity, ion mobility and charge number density were flown in recent rocket programs to investigate the high-latitude middle atmosphere. The instruments were launched in two coordinated programs (Aurorozone I and II) at Poker Flat, Alaska to study the effects of auroral energetics on electrical parameters and in a solar eclipse rocket program at Red Lake, Canada. The design of the Gerdien condenser instrumentation for the Aurorozone II program and the solar eclipse program is considered. In addition, electrical parameters measured for the two auroral programs are presented and discussed. The initial results from the measurements indicate that high-latitude middle atmosphere electrical parameters are strongly influenced by the auroral energetics.

TABLE OF CONTENTS

TABLE OF CONTENTS (cont'd)

LIST OF TABLES

LIST OF FIGURES

LIST OF FIGURES (cont'd)

LIST OF FIGURES (cont'd)

CHAPTER I

INTRODUCTION

1.1 Middle Atmosphere Ionization Sources

The middle atmosphere is generally considered to include the stratosphere, mesosphere and lower thermosphere. In altitude, this is the region of the atmosphere between approximately 15 km and 100 km. In situ measurements of middle atmosphere parameters are largely accomplished using sounding rockets since most of this region is too high for balloons and too low for satellites. If the rocket-launched instrument is deployed on a parachute, the measurement is typically limited to altitudes below 90 km where the parachute becomes wind sensitive and stabilizes.

The ionization sources in this altitude region are of solar and galactic origin. Under quiescent conditions, ionization by galactic cosmic rays is the dominant source for ions in the stratosphere and lower mesosphere [Webber (1962); Velinov (1968)]. This particular source obviously shows no diurnal variation, but it is dependent on the eleven-year solar cycle with the largest cosmic ray intensities observed during the period of minimum solar activity [Pomerantz and Duggal (1974)]. Also, the galactic cosmic ray intensity is dependent on geomagnetic latitude (below 60°), with the larger values occurring at the higher latitudes.

During the daytime, solar ultraviolet radiation is an important ionization source in the mesosphere. In particular, the photoionization of nitric oxide by hydrogen Lyman-α radiation (1216 Å) is considered the dominant source for positive ions under quiescent conditions. Other daytime sources of secondary importance during quiescent conditions include the photoionization of metastable molecular oxygen ($O_2(^1\Delta g)$) by solar EUV radiation ($\lambda < 1118$ Å) and the ionization of all constituents by solar X-rays ($\lambda < 10$ Å) [Aikin (1972)].

At high latitudes, significant enhancements in ionization are observed during periods of auroral activity. Energetic electrons are an important ionization source in the mesosphere, but normally they do not penetrate into the stratosphere. The interactions between these energetic electrons and neutral species result in a second source for ions which is observed in the stratosphere; namely, ionization by bremsstrahlung X-rays [Freyer (1969); Berger, Seltzer and Maeda (1974)]. These two ionization sources associated with auroral energetics are dependent on solar activity and appear to be rather localized and variable over short periods of time. Furthermore, ground-based riometers and magnetometers indicate that these geomagnetic distrubances occur more frequently at night.

1.2 Aurorozone Rocket Programs

Two coordinated field experiments (Aurorozone I and II) were recently conducted to study the effects of auroral energetics on the high-latitude middle atmosphere. One particular objective of these programs was to determine the effects of these events on middle atmospheric electrical parameters; particularly, electrical conductivity, ion mobility and charge number density. Rocket-launched, parachute-borne Gerdien condensers for measuring these three parameters [Pedersen (1964); Rose and Widdel (1972); Conley (1974); Croskey (1976); Sagar (1976)] and blunt probes for measuring electrical conductivity [Hale (1967); Hale, Hoult and Baker (1968)] were flown in both of these programs.

The Aurorozone I rocket program was conducted during September and October 1976 at Poker Flat Research Range, Alaska (65°N, 173°W). An overview of the launch schedule for the program is shown in Table 1-1. Two Gerdien condensers (G) and four blunt probes (BP) were successfully flown during this period. In addition, measurements of temperature (D), ozone (O_3) and X-ray energy levels (NT) were obtained as part of this program. A list of supplementary ground-based measurements are also included in Table 1-1.

The Aurorozone II program occurred during March 1978 and also was conducted at Poker Flat, Alaska. A launch schedule for this rocket program is shown in Table 1-2. The Gerdien condenser was flown as part of an integrated instrument package called the "XRG (X-ray —— Gerdien condenser) payload." In addition to the Gerdien condenser

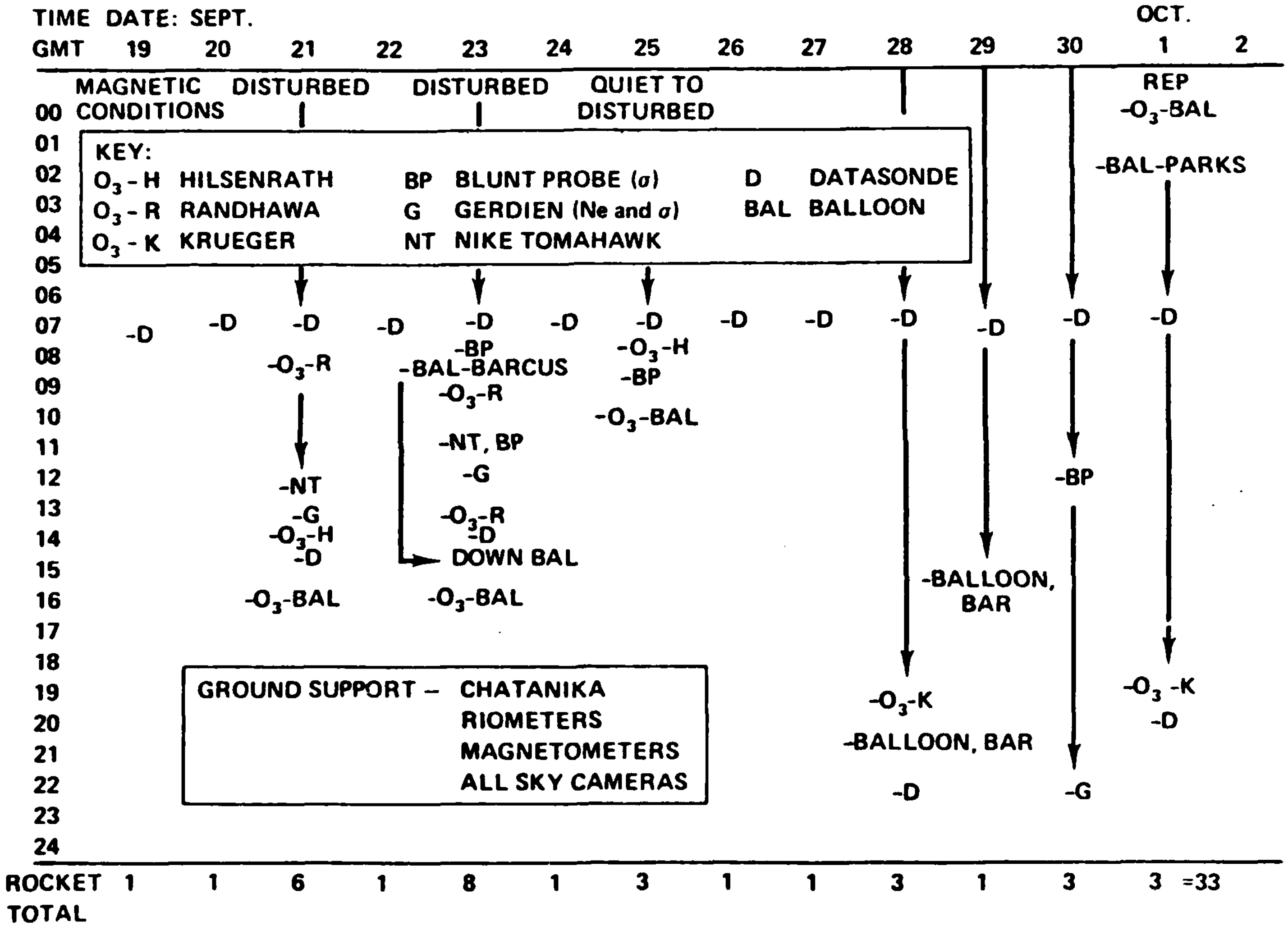

Table 1-1. Overview of the Launch Schedule (Aurorozone I)

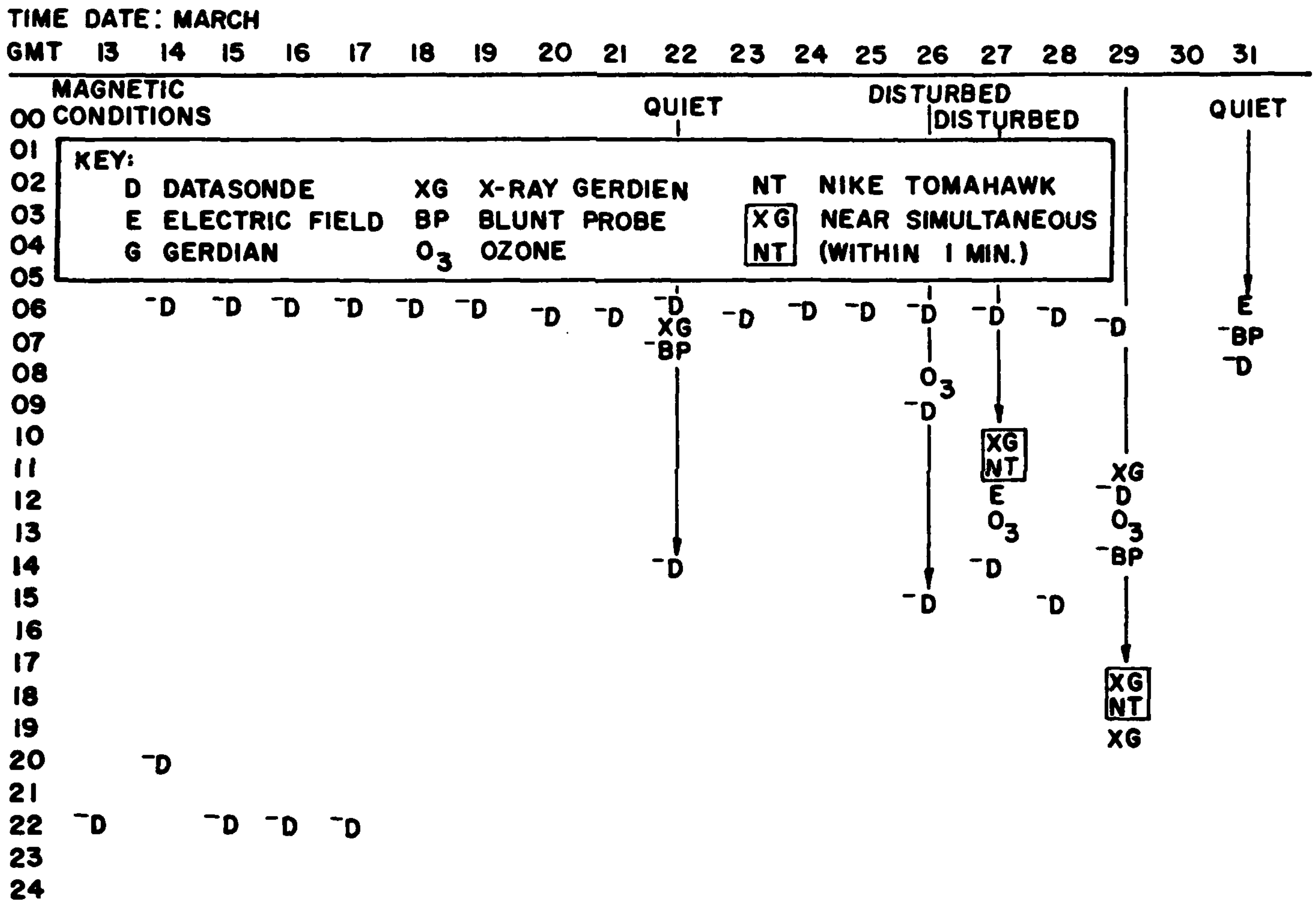

Table 1-2. Overview of the Launch Schedule (Aurorozone II)

measurements, the instrument also measured X-ray energies and vertical electric field strength. The obvious advantage of this system is the ability to simultaneously measure both the X-ray ionization source and the associated electrical parameters. The flight configuration and size of this relatively sophisticated instrument were kept small enough to be launched on a super Arcas rocket and deployed at apogee on a stabilized parachute (the disc gap band). In addition to five successful XRG payload flights, additional measurements of electrical conductivity (BP), temperature (D), ozone (O_3) and X-ray energy levels (NT) were obtained in this program.

1.3 Thesis Research

The development of the Gerdien condenser instrumentation included with the XRG payload is considered in this thesis. More recently developed circuitry designed for Gerdien condensers and a blunt probe flown in the February 1979 solar eclipse rocket is also included. Finally, the Gerdien condenser and blunt probe measurements from the Aurorozone rocket programs are presented and discussed.

CHAPTER II

GERDIEN CONDENSER OPERATION

2.1 Theory of Charged Particle Collection

A Gerdien condenser consists of a pair of concentric cylindrical electrodes, through which a well-defined axial flow geometry is developed. By proper biasing of the cylindrical electrodes and measuring the resulting collected ion current flowing through the aspirator, it is possible to determine the electrical conductivity, ion mobility and charge number density of the air sample. Determining the ion mobility and charge number density also requires that the air flow through the aspirator be known. In this section, the appropriate equations for determining these electrical parameters are presented. Further treatments of this subject are considered by Pedersen (1964), Conley (1974), Farrokh (1975), Croskey (1976) and Sagar (1976).

A schematic of the Gerdien condenser electrode configuration is shown in Figure 2-1. The collector has a radius of r_i and a length l, while the radius of the outer electrode is r_o. A uniform flow velocity $\langle v \rangle$ is assumed in the axial direction.

If the outer return electrode is assumed to be at the potential of the atmosphere, then a negative voltage on the collector will result in the collection of positive ions and vice versa. For the Gerdien condensers flown in the Aurorozone

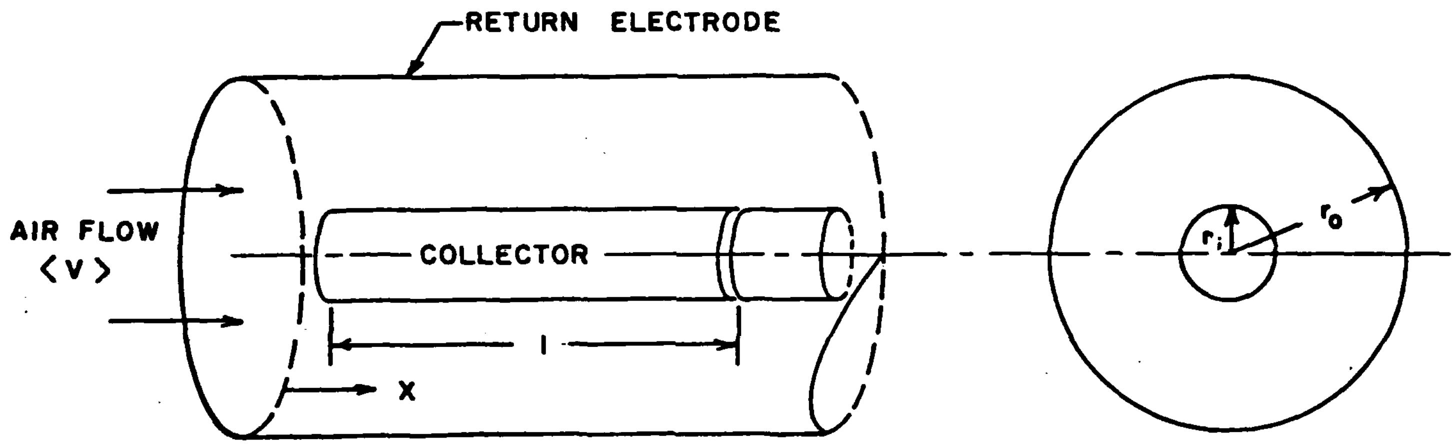

Figure 2-1. Gerdien Condenser Electrode Configuration

rocket programs, the collection voltage applied between the collector and return electrodes has the shape shown in Figure 2-2a and a period of approximately eight seconds. A possible current response to the voltage waveform as measured by the collector is shown in Figure 2-2b.

If we start at the origin (V = 0) and consider the collection voltage being swept negatively, the initial slope of the corresponding positive ion current response is proportional to the total positive conductivity σ_{+1}:

$$\sigma_{+1} = \frac{\ln(r_o/r_i)}{2\pi l} \frac{dI+}{dV}; \; 0<t<t_{+1} \qquad (2\text{-}1)$$

where

$$\sigma_{+1} = \sum_{m=1}^{M} N_{+m} \, e \, k_{+m} \qquad (2\text{-}2)$$

In this equation, we are assuming that there are M unique positive ion mobility groups. Actually in the example of Figure 2-2b, we are considering the case of M=3.

The break in the positive ion current response at t_{+1} indicates that all of the ions of the highest mobility group k_{+1} are collected from the air sample. The collection voltage value V_{+1} at t_{+1} is the minimum value for which a positive ion of mobility k_{+1} entering the aspirator at a radial distance $(r_o - r_i)$ from the collector can still be collected. The equation for V_{+1} is

$$V_{+1} = - \frac{(r_o^2 - r_i^2) \langle v \rangle \ln(r_o/r_i)}{2 \, k_{+1} \, l} \qquad (2\text{-}3)$$

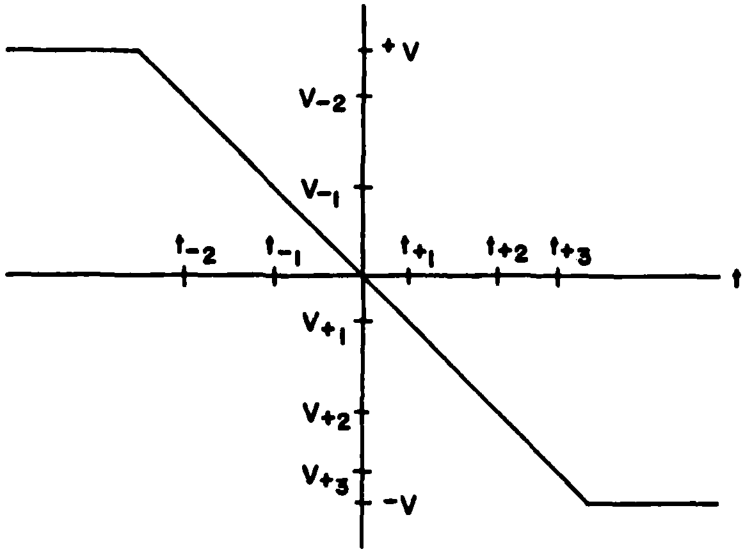

Figure 2-2a. Gerdien Condenser Collection (sweep) Voltage Waveform

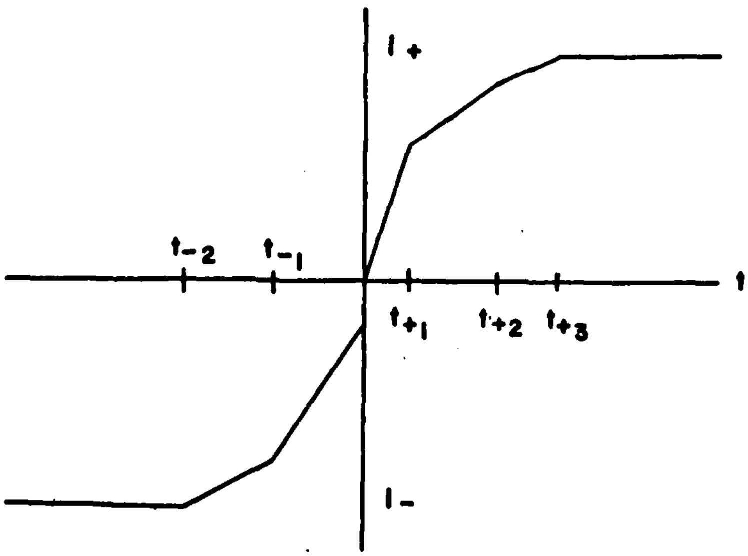

Figure 2-2b. Gerdien Condenser Current Response Characteristic (Example)

Thus, solving for the collection voltage at t_{+1} enables us to determine the ion mobility value k_{+1}.

Since at large negative collection voltages all the ions of mobility k_{+1} will be collected from the air sample, there is no further increase in I_+ associated with this mobility group. The slope between t_{+1} and t_{+2} is therefore relatively smaller in value and is used to determine the partial conductivity

$$\sigma_{+2} = \sum_{m=2}^{M} N_{+m}\ e\ k_{+m} \tag{2-4}$$

This development continues with each additional breakpoint indicating when the next highest mobility group is completely collected from the air sample. The general equations to determine the values of the different ion mobility groups and their corresponding concentrations are:

$$k_{+m} = \frac{(r_o{}^2 - r_i{}^2)\ \langle v\rangle \ln(r_o/r_i)}{2\ V_{+m} l} \tag{2-5}$$

$$N_{+m} = \frac{\sigma_{+m} - \sigma_{+(m+1)}}{e\ k_{+m}} \tag{2-6}$$

In reexamining Figure 2-2, there are several points worth noting. First, for a sufficiently large negative collection voltage such that all positive ions are collected from the air sample, the current response becomes flat for increasing voltage. This is the saturation mode of operation and the positive ion saturation current is simply

$$I_{+s} = \pi(r_o^2 - r_i^2)\ N_+\ q\langle v\rangle \tag{2-7}$$

Under the saturation condition, the positive ion current value may be used to determine the total positive ion number density.

Secondly, the development for obtaining the equations describing the collection of negative charge species is similar. If free electrons are present as shown in Figure 2-2b, their mobility values are so much greater that there appears at the origin approximately a step increase in current. The I-V response of Figure 2-2b shows the collection of electrons and two different negative ion mobility groups. The corresponding equations for determining total negative conductivity (σ_{-1}) and the mobility and density values of ion mobility group k_{-p} are respectively:

$$\sigma_{-1} = \frac{\ln(r_o/r_i)}{2\pi l}\ \frac{dI_-}{d};\ t_{1-}<t<0 \tag{2-8}$$

where

$$\sigma_{-1} = \sum_{p=1}^{P} N_{-p}\ e\ k_{-p} \tag{2-9}$$

$$k_{-p} = \frac{(r_o^2 - r_i^2)\ \langle v\rangle \ln(r_o/r_i)}{2\ V_{-p} l} \tag{2-10}$$

$$N_{-p} = \frac{\sigma_{-p} - \sigma_{-(p+1)}}{e\ k_{-p}} \tag{2-11}$$

In writing these equations, it is assumed there are P different mobility groups for the negative charge species.

Finally, if relatively immobile ions are present in an air sample, the actual range of collection voltages for the Gerdien condenser might not be sufficient to achieve saturation. If this is the case, then one is unable to determine the values for these less mobile groups which are not saturated out nor the total ion density.

2.2 The Gerdien Condenser Launch

The Gerdien condensers in the Aurorozone I and II rocket programs were flown on super Arcas rockets. Prior to the launch, the instrument is calibrated by connecting a known-value resistor (R_{CAL}) in parallel with the Gerdien condenser electrodes. The electrometer's output response when the collection voltage waveform is applied across the resistor is received through the telemetry system and recorded on magnetic tape.

The actual in-flight measurements are obtained after the payload separates from the rocket at apogee and is descending on a stabilizied parachute system. The telemetered in-flight data are received by a ground-based system and recorded on magnetic tape.

The probe's position and velocity during the flight are obtained by using a radar. For the recent Gerdien condenser flights conducted during the solar eclipse, however, a transponder was included with the transmitter system to provide ranging information. The ranging data along with the azimuth and elevation angles from a GMD-4 telemetry receiving system were then used to determine the probe's position and velocity. This particular transponder system was used for rocket flights when radar tracking was not available.

Upon completion of the rocket flight, the data are played back onto a strip chart for reduction. The actual equation used for scaling the data is dependent on the probe's electronics, and is included in Chapter 4.

CHAPTER III

INSTRUMENTATION DESIGN

3.1 XRG Payload Configuration

The sensor configuration for the XRG payload is shown in Figure 3-1. As discussed previously, the XRG payload combined a Gerdien condenser with an X-ray scintillation detector and an electric field sensor. When the instrument package is deployed on a parachute, the Gerdien condenser is oriented downward. The air flow through the aspirator is determined from the instrument's descent velocity which is measured by a ground-based radar. Payload orientation is determined using a two-axis magnetometer.

In flight, the aperture for the X-ray scintillation detector is directed upward. The detector uses sodium iodide (NaI) crystals which floresce when impacted by X-rays. The resulting photons are detected by a photomultiplier tube. The X-ray energies are measured in four different ranges: 5-10 keV; 10-20 keV; 20-40 keV; and greater than 40 keV. In addition, a Geiger-Mueller tube for measuring energetic electrons and monitoring cosmic rays was included.

The electric field sensor consists of a probe mounted at the base of the parachute and connected to the payload body by a two-meter wire which spirals around the parachute lanyard. The vertical electric field is determined by measuring the voltage between the probe and the payload body.

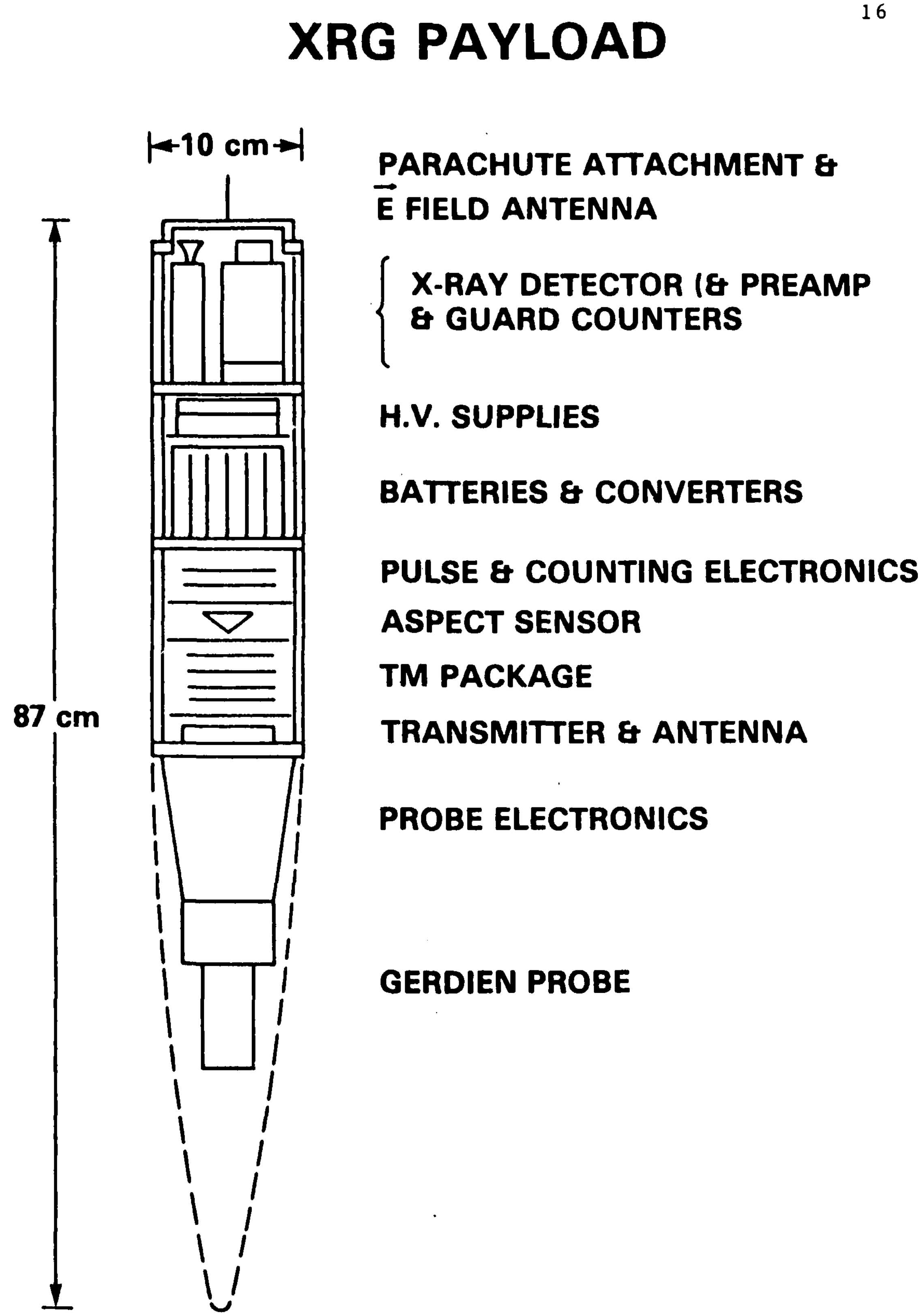

Figure 3-1. XRG Payload Configuration

The transmitter and electronics are housed in a 10.2 cm diameter fiber glass cylinder which has a 1680 MHz micro-strip-type antenna photoetche on the outside surface. The PCM encoding system provides a bi-phase level output with nine words per frame and eight bits per word at a bit rate of 8k bits/second. The encoder input accepts a 0-5 V analog voltage waveform. All of the electronics are powered by six PM1 silver cell batteries.

3.2 Gerdien Condenser Design for the XRG Payload

A sketch of the electronics system associated with the Gerdien condenser is shown in Figure 3-2. The sweep voltage waveform provides a known collection voltage waveform to the guard portion of the inner collecting electrode. By connecting the guard electrode to the electrometer's noninverting input terminal and the collector to the inverting input terminal, the collector is also "virtually" at the sweep voltage potential. It was necessary to bias the outside skin of the XRG payload at ground potential in order to keep the probe's electronics compatible with the X-ray detector and the electric field probe.

A circuit diagram for the sweep voltage generator is shown in Figure 3-3. The waveform shown in Figure 3-3 is obtained by using an astable multivibrator followed by a constant current run-down circuit. The sweep voltage obtained at the output of the LM 264 operational amplifier follower is connected to both the noninverting terminal of

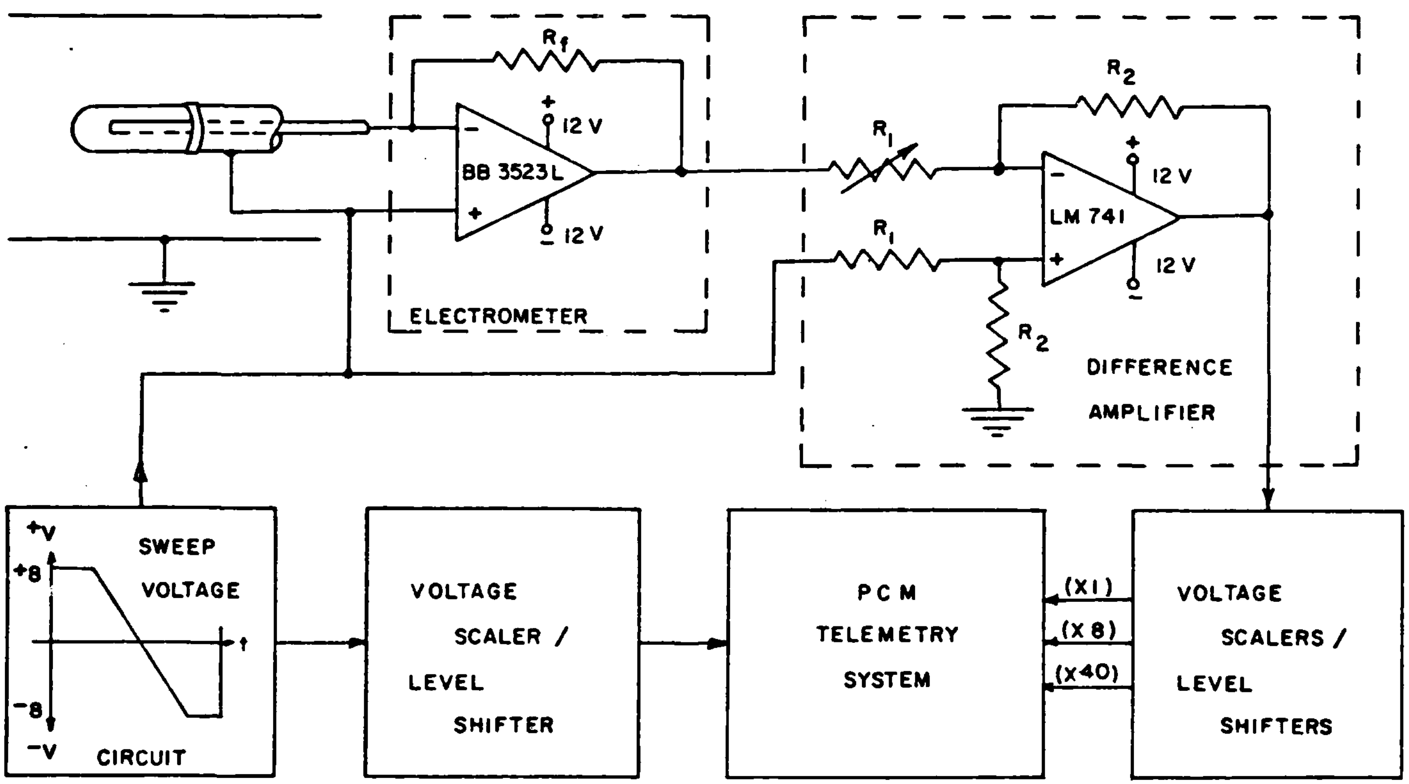

Figure 3-2. Gerdien Condenser Electronic System (Aurorozone II)

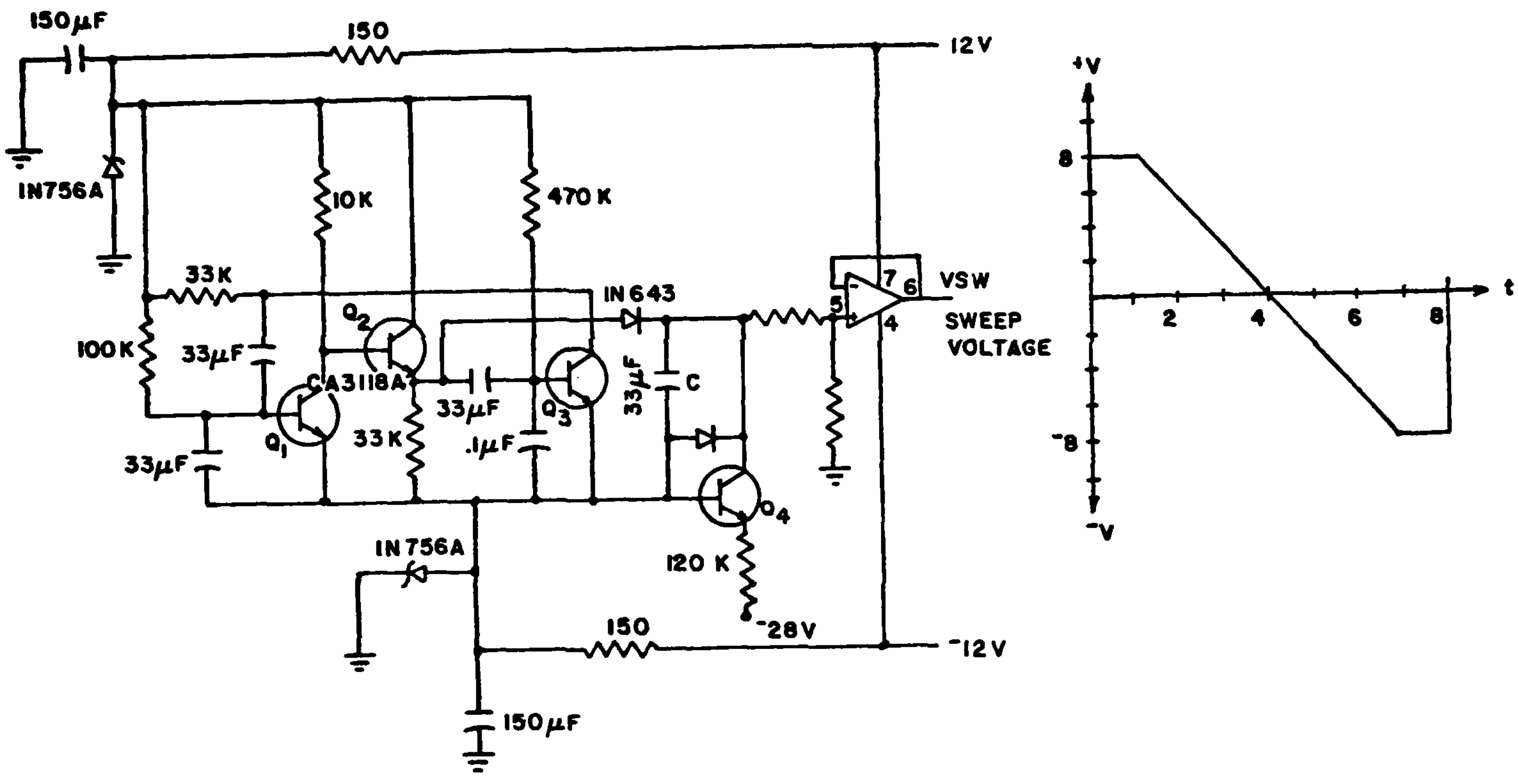

Figure 3-3. Sweep Voltage Circuit (Aurorozone II)

the electrometer and a voltage difference amplifier. Regulated voltage values of ± 12 V were supplied to the sweep voltage circuit using a LM 126H voltage regulator.

The current of charged particles drawn to the collector is measured by an electrometer (Figure 3-2). The electrometer for the XRG payload uses a Burr-Brown 3523L operational amplifier which has a nominal input bias current of 0.1 pA and a 100 dB common-mode rejection ratio. A Victoreen MOX-400A resistor of value 1×10^9 ohms is used in the feedback path. For supply voltages of ± 12 V and a common-mode voltage (the sweep voltage) ranging between ± 8 V, the electrometer's measurement range is approximately ± (2-3) nA.

After differencing the sweep voltage from the electrometer output signal, the data waveform is fed to three parallel voltage scalers/level shifters (Figure 3-4). The level shifting produces a 0-5 V analog signal compatible with the PCM encoder. The scaling operation results in data current ranges of approximately: ± 2 x 1.0 nA (Channel 1); ± 2 x 0.125 nA (Channel 2) and ± 2 x 0.025 nA (Channel 3). The multi-channel telemetry capability of the XRG payload is advantageous in that it enhances the Gerdien condenser's measurement range to approximately four decades. The two less sensitive current measurements were allocated separate telemetry channels while the most sensitive current channel was assigned to a commutated channel. In

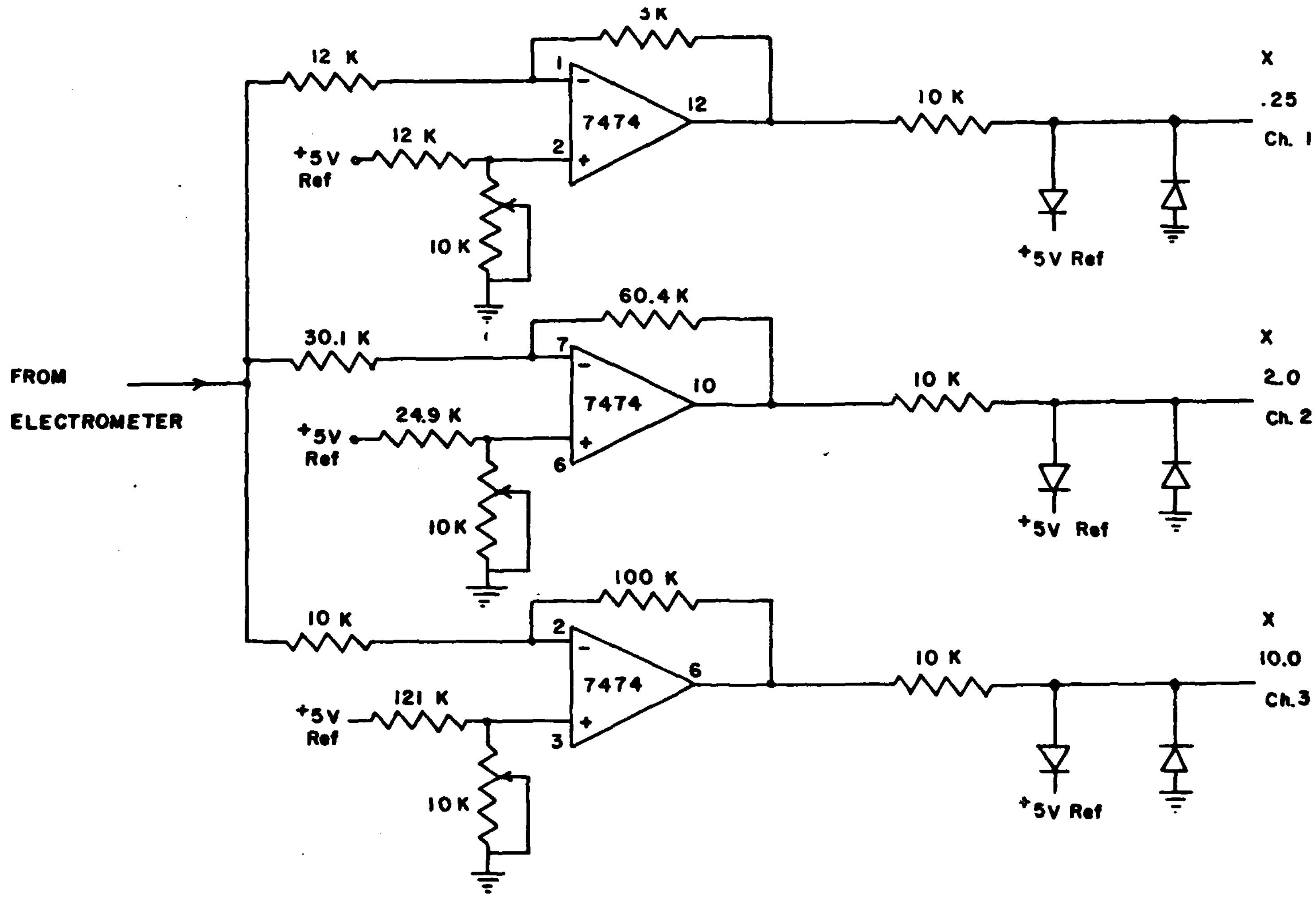

Figure 3-4. Voltage Scalers/Level Shifters (Aurorozone II)

addition, monitoring of the sweep voltage and the battery voltage levels was also telemetered on the commutated channel.

3.3 Solar Eclipse Payload Configuration

The Gerdien condenser designed for the February 1979 solar eclipse rocket program included a magnetometer and PCM encoder similar to those used with the XRG payload. The remote launch site necessitated the inclusion of a Space Data Corporation PWN-10A 403 MHz transponder for ranging information. The transponder uses an 83 kHz pulse waveform to modulate the plate voltage of the RCA 4048V3 1680 MHz transmitter. The antenna housing for this payload was also a 10.2 cm diameter fiber glass cylinder with strip line antennas for both receiving the upleg 403 MHz signal and transmitting at 1680 MHz.

The relatively smaller payload length (48.9 cm) and weight (2.930 kg) afforded a somewhat higher flight apogee (nominally 80 km) where the payload separated from the super Arcas rocket and was deployed on a stabilized parachute (either a disc gap band or starrute).

At the time of this writing, only the launch dates and times are known for the Gerdien condensers and blunt probes flown in the solar eclipse rocket program. These launch parameters are listed in Table 3-1.

GERDIEN CONDENSER/BLUNT PROBE LAUNCH PARAMETERS FOR THE SOLAR ECLIPSE

ROCKET PROGRAM AT RED LAKE, CANADA (51°N, 94°W)

Launch		Instrument	Rocket	Comments
Date (1979)	Time (CST)			
Feb. 24	1122	Blunt Probe	Super Arcas	Pre eclipse
Feb. 25	1130	Gerdien Condenser	Super Arcas	Pre eclipse
Feb. 26	1053	Gerdien Condenser	Super Arcas	Eclipse Totality
Feb. 26	1138	Gerdien Condenser	Super Arcas	Totality + 45 min.
Feb. 26	2130	Gerdien Condenser	Super Arcas	Nighttime
Feb. 26	2240	Blunt Probe	Super Loki	Nighttime
Feb. 27	0706	Gerdien Condenser	Super Arcas	Sunrise
Feb. 27	0840	Blunt Probe	Super Loke	Morning

Table 3-1

3.4 Gerdien Condenser Design for the Solar Eclipse Payload

A schematic for the Gerdien condenser electronic system is shown in Figure 3-5. The sweep voltage waveform is similar in shape but has approximately twice the range as that used for the XRG payload. The noticeable difference in operation is that the return electrode and payload skin are biased at the sweep voltage and the inner guard electrode is grounded, thus avoiding the need for a voltage difference amplifier following the electrometer. The electrometer output is connected directly to three parallel voltage scalers/level shifters which in turn, are connected to individual channels of the PCM telemetry system. As previously discussed, the PCM encoder and transmitter system —— excluding the transponder —— are similar to these flown on the XRG payload.

The sweep voltage circuit is a different design as shown in Figure 3-6. This particular circuit produces a periodic voltage waveform with negative-going ramp that is limited by the two supply voltages, in this case ± 16 V.

For the operational amplifiers (op amps) numbered one to four, a LM224 quad op amp was used. Op amp number 5 is a LM 741. The circuitry with op amp 1 forms a square wave generator which can be monitored at P1. The 2N3821 silicon n-channel junction field-effect transistor (JFET) and op amp 3 form a constant current sink for C_2. Op amp 2 is used as a comparator to give the negative-going voltage

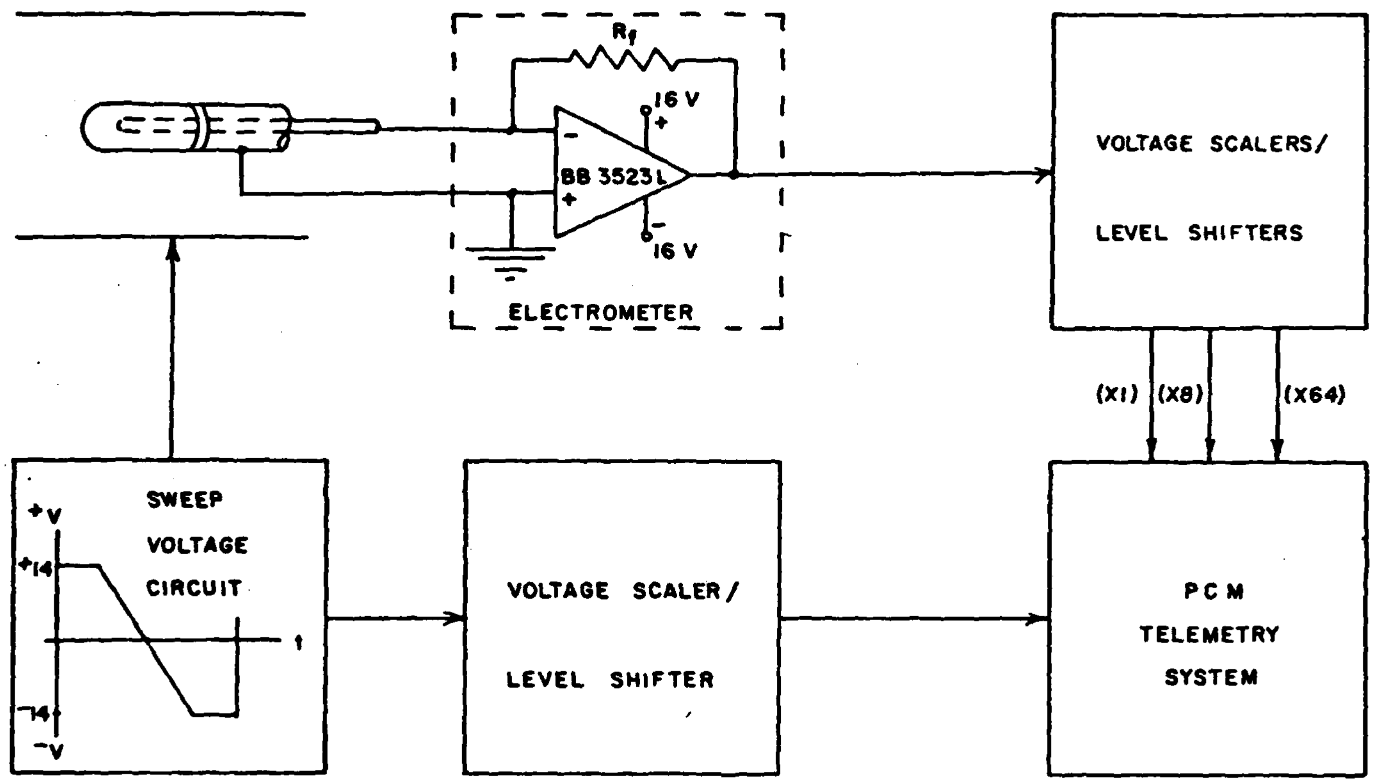

Figure 3-5. Gerdien Condenser Electronic System (Solar Eclipse)

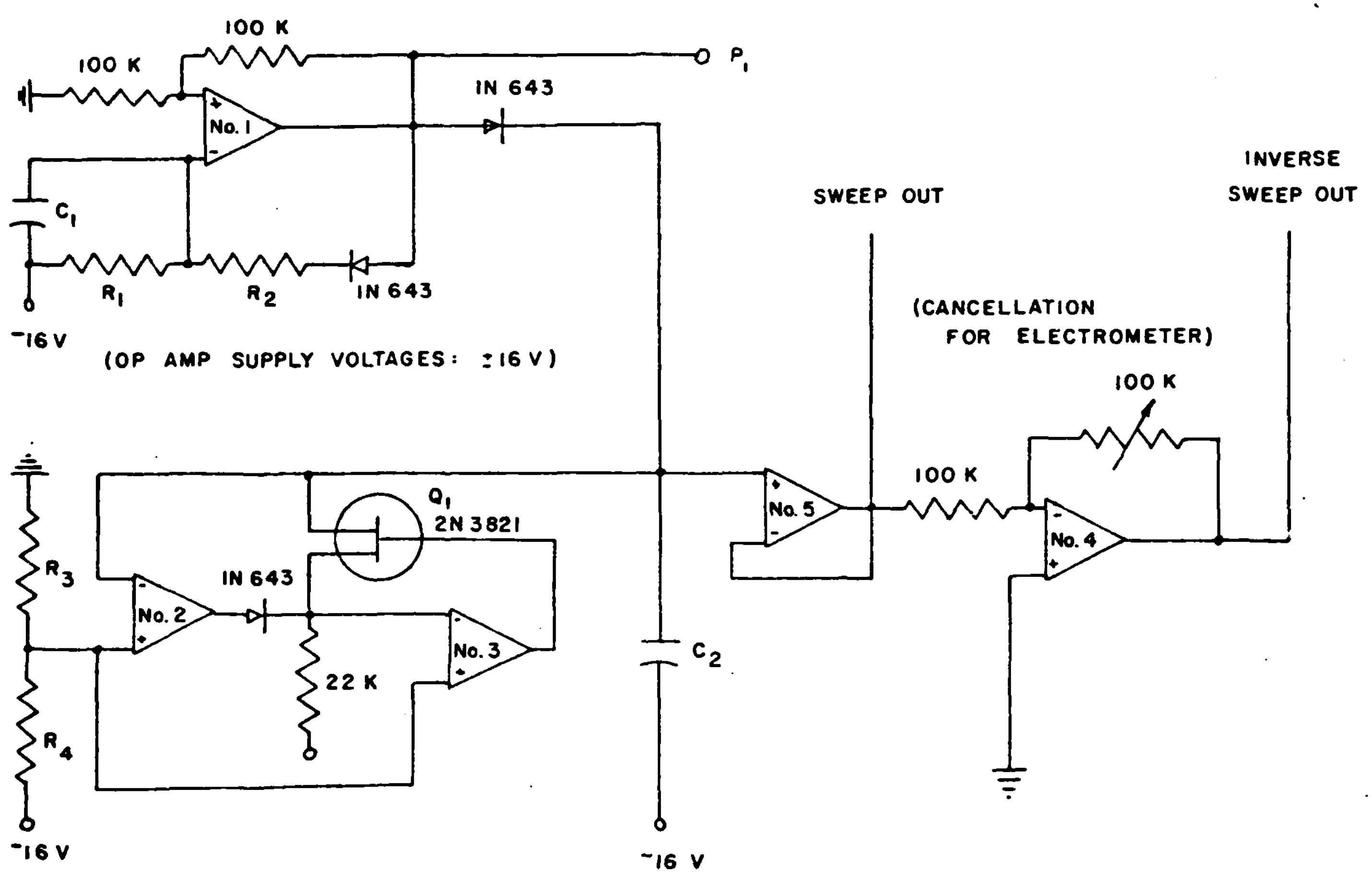

Figure 3-6. Sweep Voltage Circuit (Solar Eclipse)

ramp a hard limit at approximately -15 V. The output of the LM741 op amp follower is connected to the return electrode and it also drives an op amp inverter (number 4) and another LM 741 op amp follower (not shown). This additional op amp follower biases the payload skin at the sweep voltage and avoids possible r-f noise leaking back to the initial sweep output. The inverted sweep voltage waveform is used for displacement current cancellation at the electrometer input.

The electrometer (Figure 3-5) uses the Burr-Brown 3523L operational amplifier with a Victoreen Hi-Meg feedback resistor (R_f) of either 5×10^9, 1×10^{10} or 2×10^{10} ohms. The current measurement range is approximately ($\pm 15/R_f$) amperes. This particular current range is allocated to one data channel, with current ranges 8 and 64 times more sensitive inputted to other separate data channels.

The Gerdien condenser displacement current associated with the sweep voltage is large enough to saturate the most sensitive current measurement range. Therefore, a scaled inverted sweep voltage connected to a low leakage capacitor is also supplied to the electrometer input to cancel the other displacement current component. The very sensitive electrometer and the appreciable electrode capacitance ($\simeq$ 2 pF) make it necessary to strongly filter any noise riding on the sweep voltage, thus reducing possible noise displacement current to the electrometer input.

The voltage scalers/level shifters shown in Figure 3-7 set the current range sensitivities and produce voltage levels (0-5 V) compatible with the PCM encoder.

3.5 Gerdien Condenser Mechanical Design

The mechanical design of the Gerdien condenser for the XRG and solar eclipse payloads is similar. A drawing of the electrode configuration is shown in Figure 3-8.

The Gerdien condenser electrodes consist of an inner collector with a guard electrode and an outer return electrode. The collector and guard are copper, and are separated and alligned by a nylon spacer. The collector's outside diameter is 1.587 cm and its length is 6.350 cm. A brass threaded rod connects the collector and provides an electrical conducting path to the electrometer. The guard reduces fringing of the electric field at the joined end of the collector and shields the collector's conducting rod from r-f pickup and photoemission from the sun. The collector also needs to be shielded from the sun by the return electrode to avoid possible photoemission. The outer return electrode is aluminium and has an inside diameter of 7.46 cm and a wall thickness of 0.079 cm. The free space capacitance of this concentric electrode configuration is approximately 2 pF.

The delrin piece to which the return electrode is connected is flared to improve the air flow geometry through the aspirator. The electrometer is housed within the

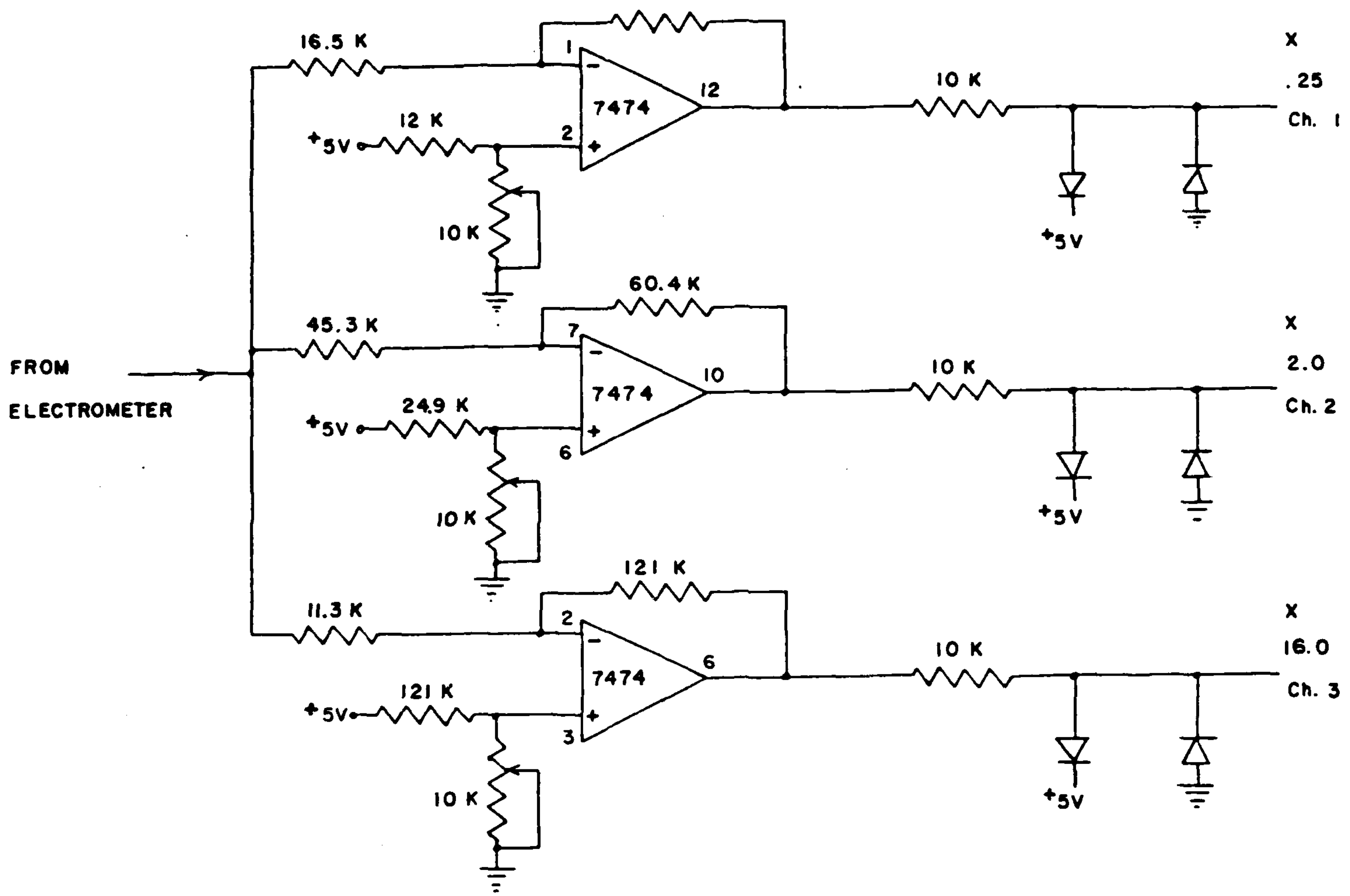

Figure 3-7. Voltage Scalers/Level Shifters (Solar Eclipse)

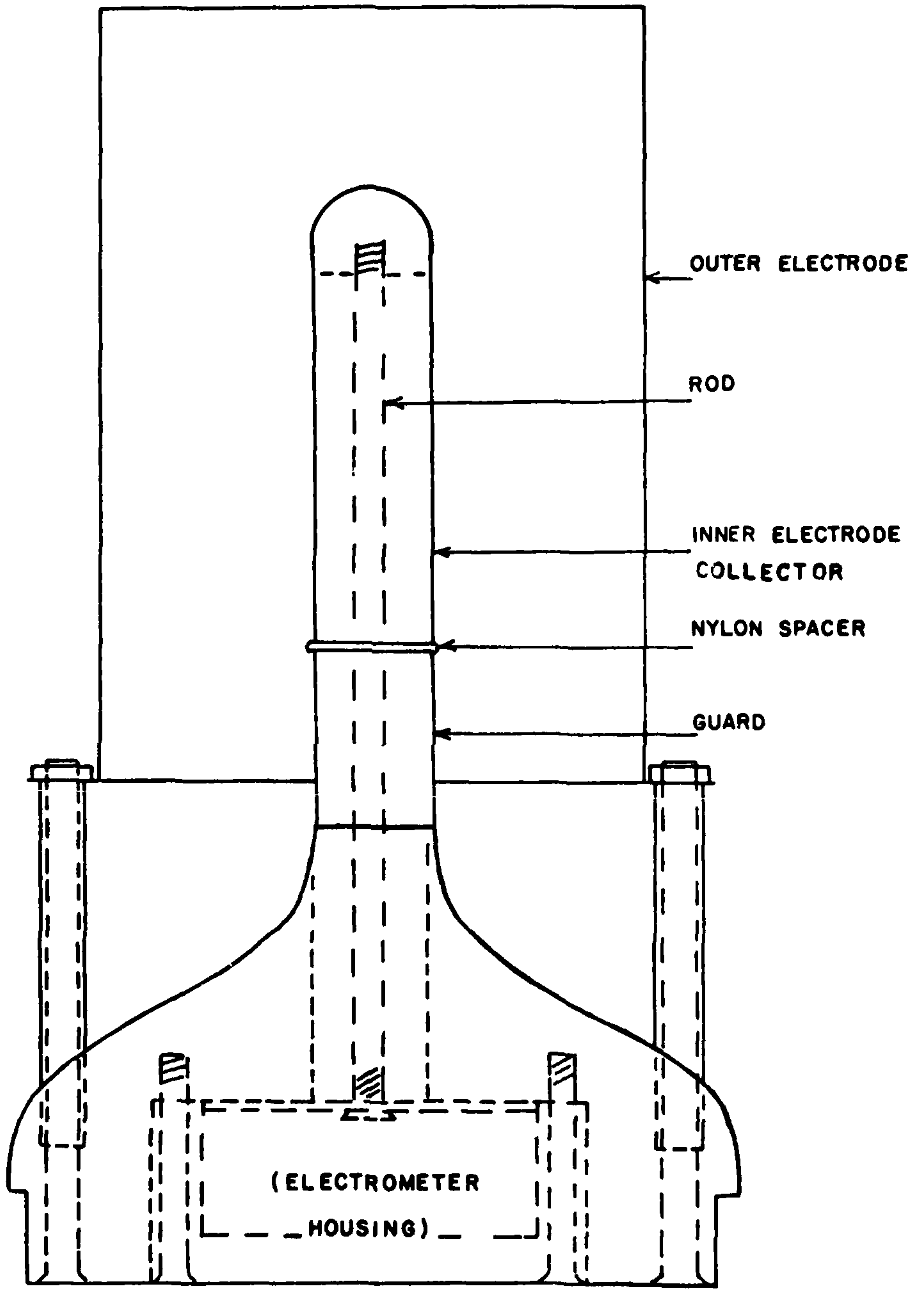

Figure 3-8. Gerdien Condenser Probe Configuration

delrin piece, with the electrometer circuitry contained inside an aluminum cup. The aluminum cup shields the electrometer circuitry from possible noise, and electrical connections to the circuitry are made with Erie-003 rfi filters.

The flared delrin piece fits to the fiber glass antenna housing described earlier. Three bolts in the axial direction align the printed circuit boards inside the antenna housing and keep the entire instrument package together.

CHAPTER IV

HIGH-LATITUDE MIDDLE ATMOSPHERE ELECTRICAL PARAMETERS

Middle atmosphere electrical parameters measured in the Aurorozone I and II programs are presented in this chapter. The equation for reducing the Gerdien condenser electrical conductivity data, which is dependent on the electronics and the preflight calibration, is also presented.

4.1 Aurorozone I Rocket Program

A list of the launch parameters for the Aurorozone I rocket instruments measuring electrical conductivity is presented in Table 4-1. Although the emphasis of this research is concerned with the Gerdien condenser flights, electrical conductivity data from the parachute-borne blunt probes are included since these measurements are relevant to future discussion.

The electrode biasing scheme for the Aurorozone I Gerdien condensers (and also for the recent solar eclipse payloads —see Figure 3-5) involved biasing the outer return electrode and payload skin at the sweep voltage with reference to the inner guard electrode (and virtually the collector). Applying Equation 2-1 and 2-8 to this probe electronics scheme, the equation for determining the positive and negative electrical conductivity values is

$$\sigma_{\pm} = \frac{\ln(r_o/r_i)}{2\ l\pi R_{CAL}} \quad \frac{(dV_{\pm}/dt)_{DATA}}{(dV/dt)_{CAL}} \qquad (4\text{-}1)$$

GERDIEN CONDENSER/BLUNT PROBE LAUNCH PARAMETERS FOR THE AURORAZONE I

ROCKET PROGRAM AT POKER FLAT, ALASKA (65°N, 173°W)

Date (1976)	Time (AST)	Instrument	Rocket	Geomagnetic Conditions
Sept. 21	0324	Gerdien Condenser	Super Arcas	Disturbed
Sept. 22	2200	Blunt Probe	Super Loki	Quiet
Sept. 23	0137	Blunt Probe	Super Loki	Disturbed
Sept. 23	0220	Gerdien Condenser	Super Arcas	Disturbed
Sept. 24	2254	Blunt Probe	Super Loki	Disturbed
Sept. 30	0251	Blunt Probe	Super Loki	Quiet

Table 4-1

In this equation, r_o, r_i and l are Gerdien condenser probe dimensions as defined in Chapter 3. The calibration resistor value is R_{CAL}. Finally, the expressions $(dV\pm/dt)_{DATA}$ and $(dV/dt)_{CAL}$ are the time rates of change of the electrometer output voltage in flight and during preflight calibration, respectively. The procedure for obtaining these waveforms is discussed in Section 2.2.

The electrical conductivity data for the Gerdien condenser flown at 0324 AST on September 21, 1976 are plotted in Figure 4-1. The corresponding positive ion mobility and charge number density values for this flight, which were scaled using Equations 2-5 and 2-6, are plotted in Figures 4-2 and 4-3, respectively.

Electrical conductivity values for the blunt probes flown on September 22, 1976 at 2200 AST and September 23, 1976 at 0137 AST are shown in Figures 4-4 and 4-5, respectively.

The second Gerdien condenser flown in this program was launched on September 23, 1976 at 0220 AST. The positive conductivity, ion mobility and charge number denisty data for this rocket flight are plotted in Figures 4-6, 4-7, and 4-8, respectively.

Finally, the last two rocket payloads for measuring electrical conductivity in the Aurorozone I program were blunt probes launched on September 24, 1976 at 2254 AST and September 30, 1976 at 0251 AST. The electrical conductivity

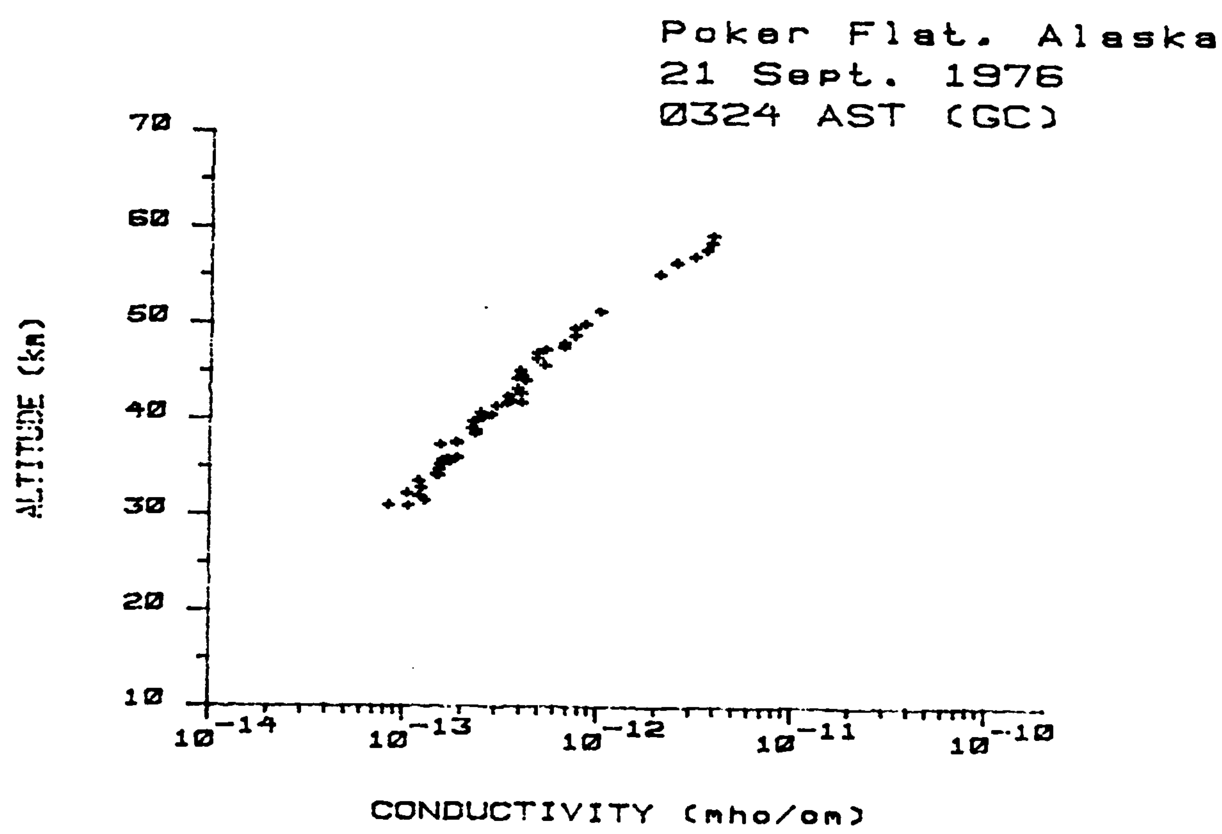

Figure 4-1. Positive Electrical Conductivity Measurements for 0324 AST on September 21, 1976

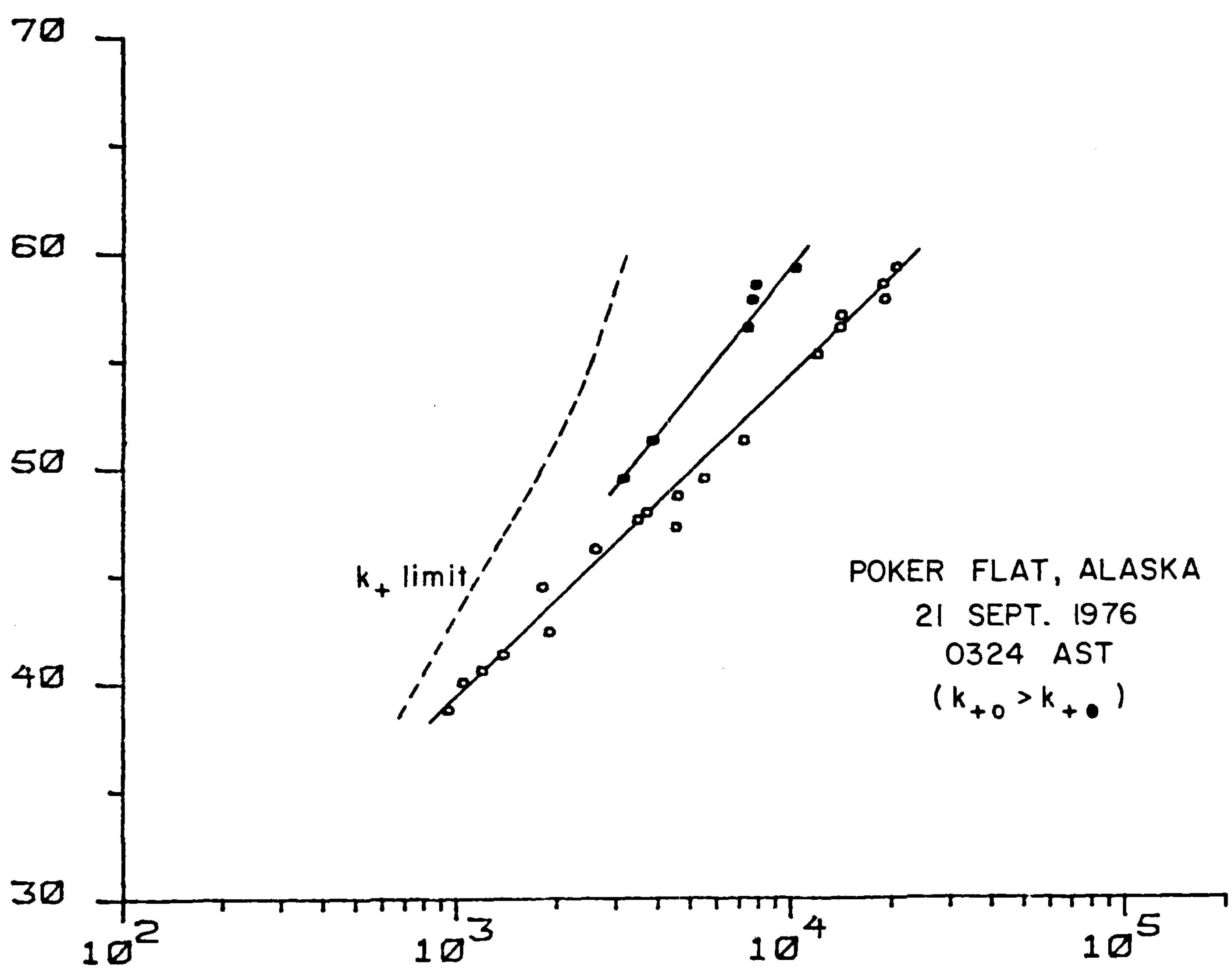

Figure 4-2. Positive Ion Mobility Measurements for 0324 AST on September 21, 1976

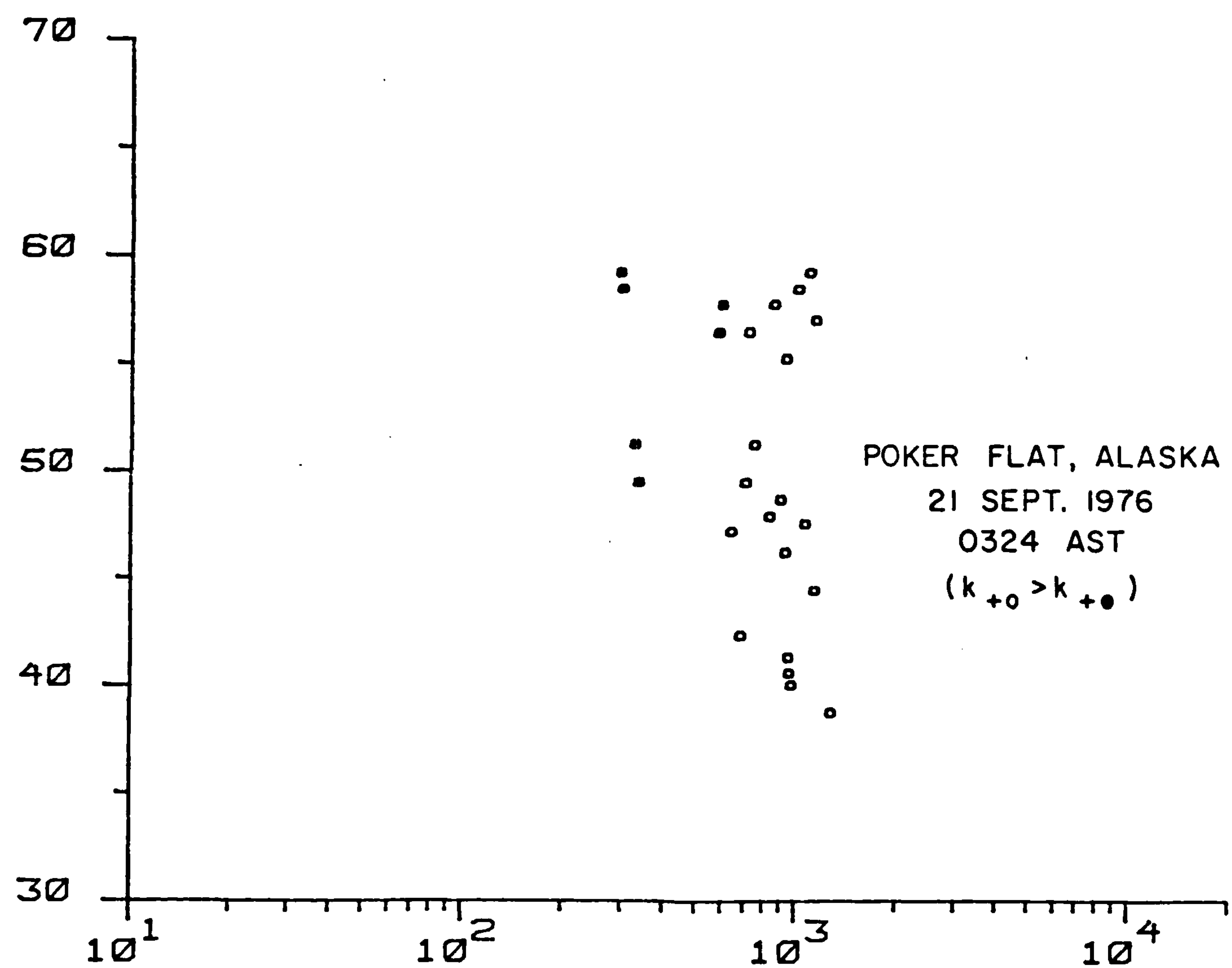

Figure 4-3. Positive Ion Number Density Measurements for 0324 AST on September 21, 1976

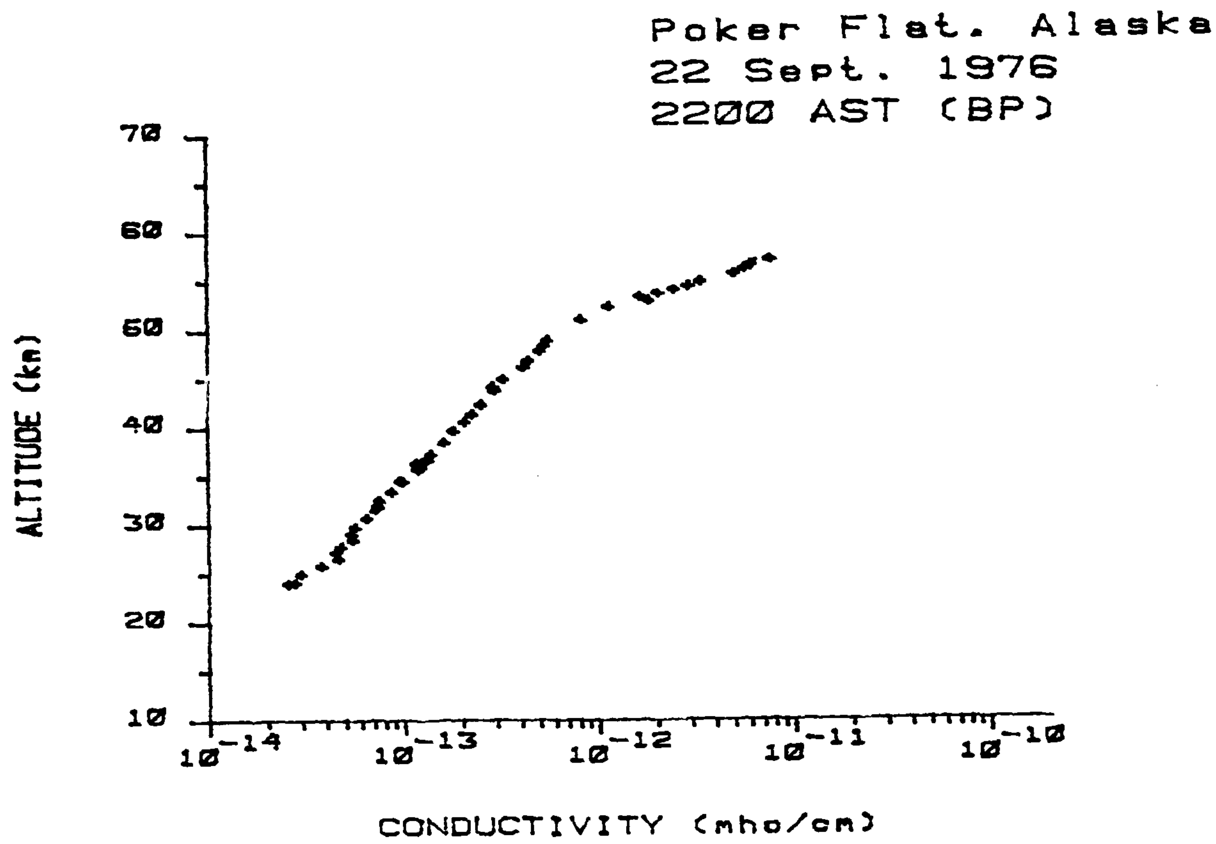

Figure 4-4. Positive Electrical Conductivity Measurements for 2200 AST on September 22, 1976

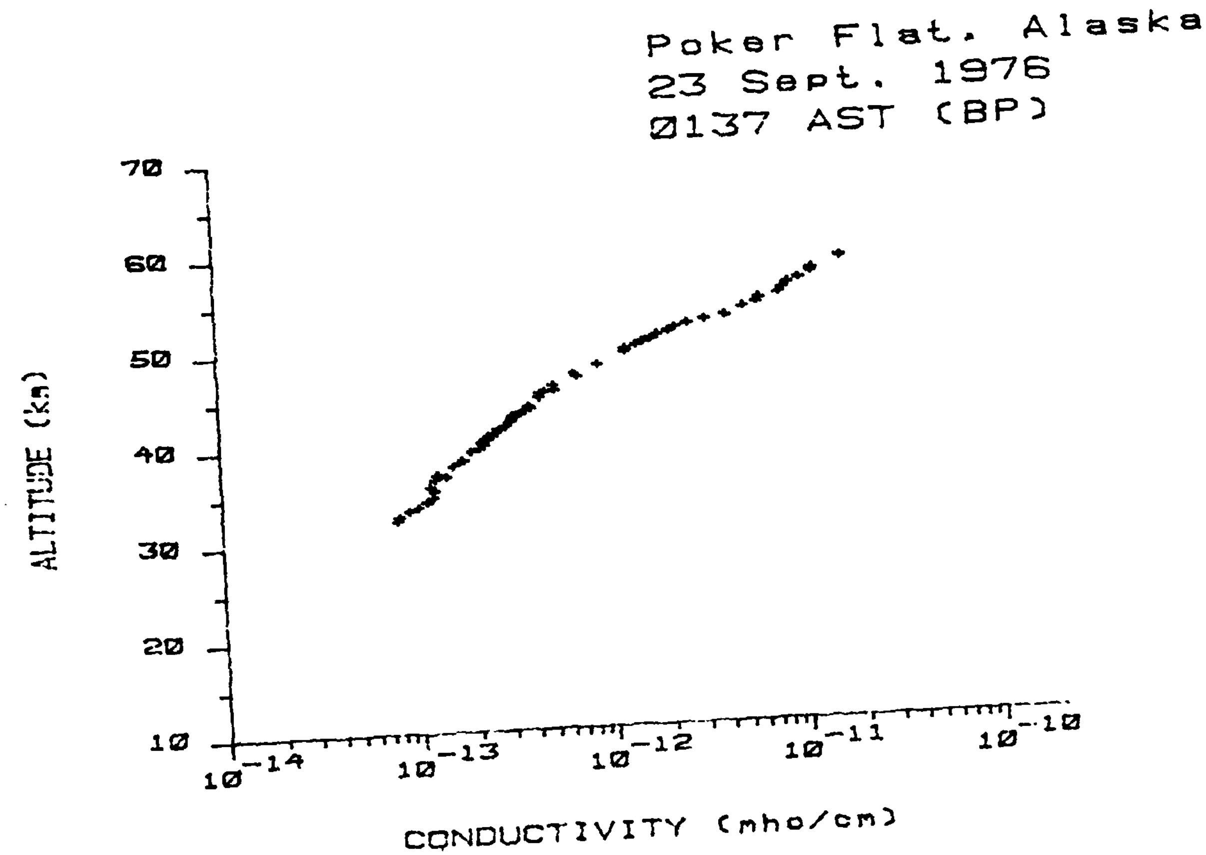

Figure 4-5. Positive Electrical Conductivity Measurements for 0137 AST on September 23, 1976

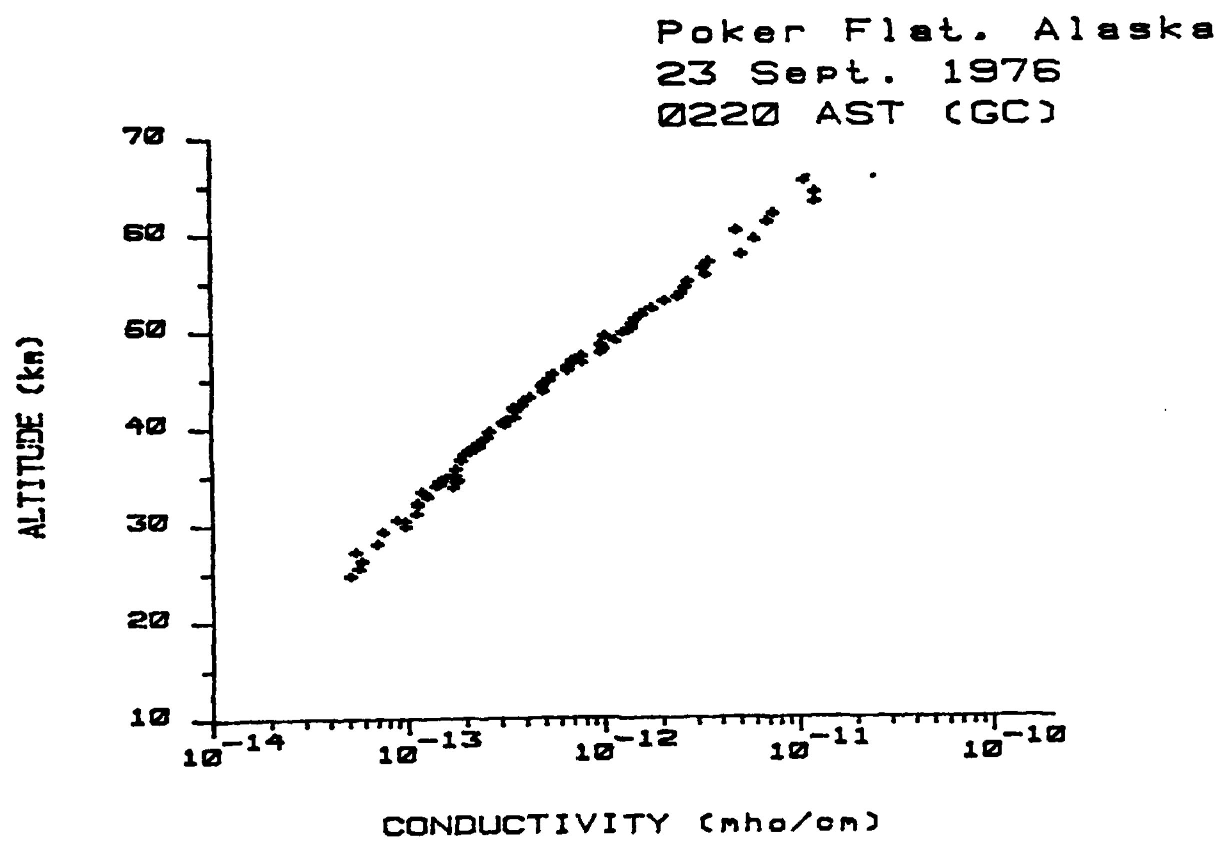

Figure 4-6. Positive Electrical Conductivity Measurements for 0220 AST on September 23, 1976

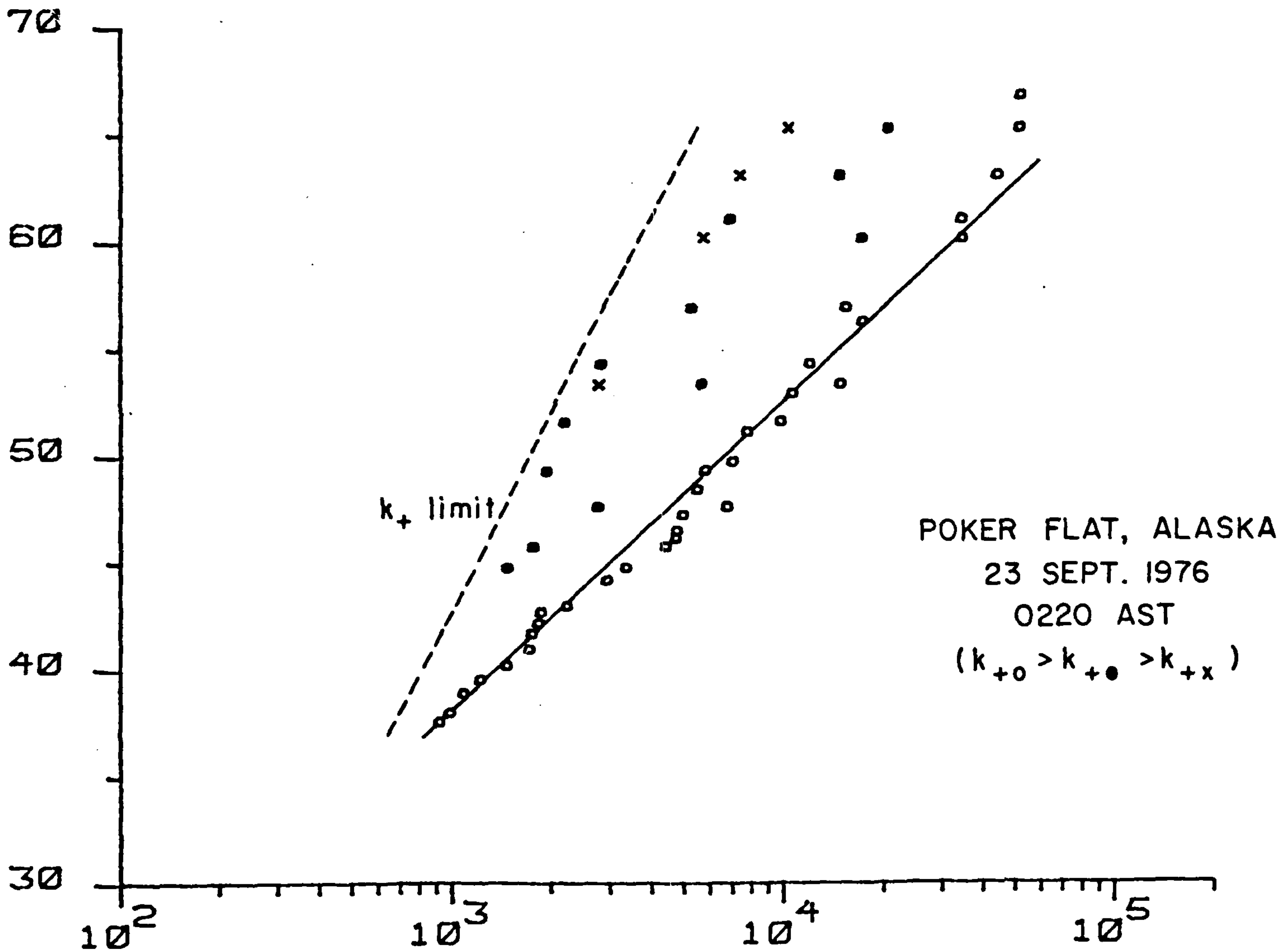

Figure 4-7. Positive Ion Mobility Measurements for 0220 AST on September 23, 1976

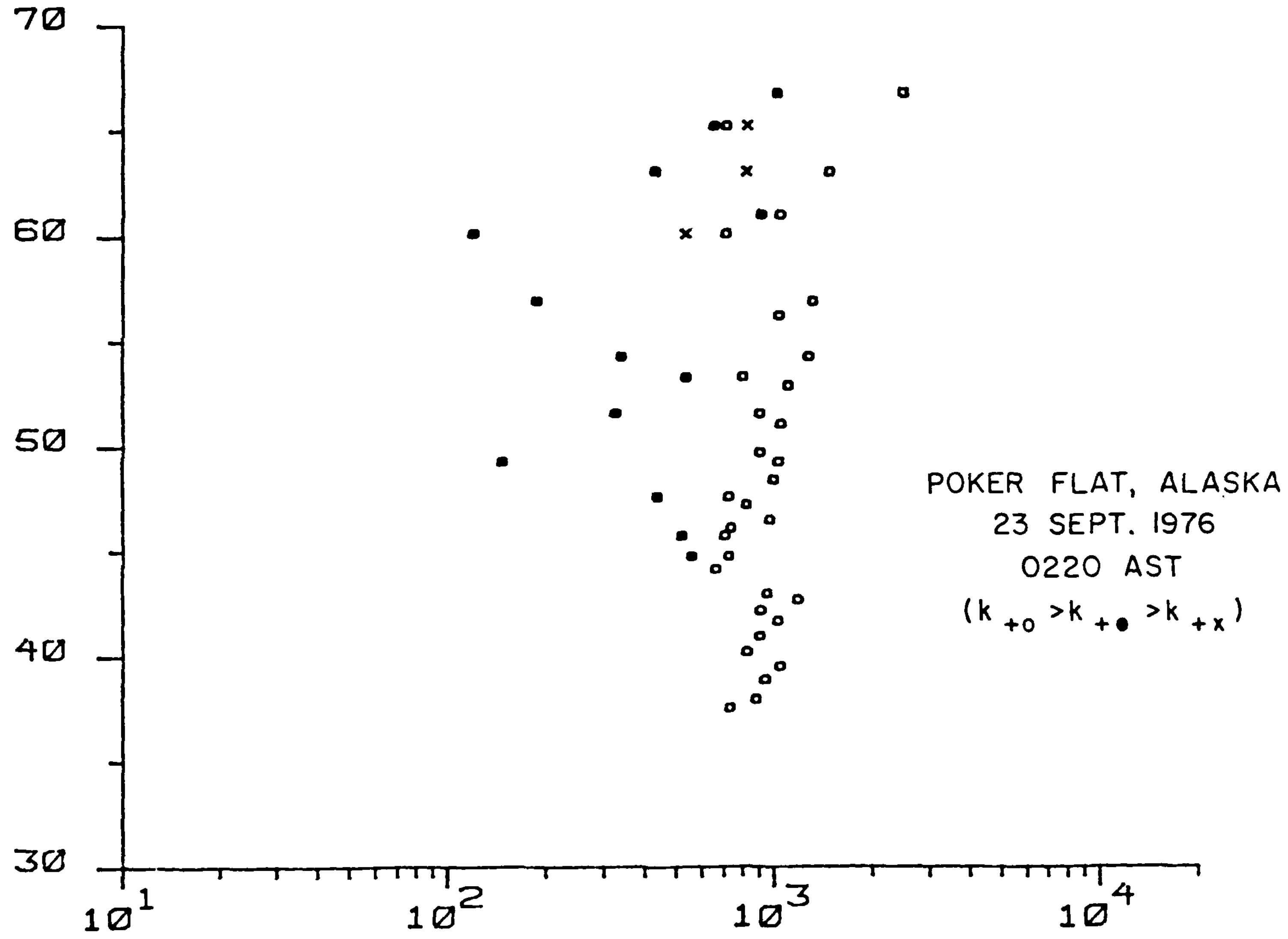

Figure 4-8. Positive Ion Number Density Measurements for 0220 AST on September 23, 1976

data from these two rocket flights are shown in Figures 4-9 and 4-10 respectively.

4.2 Aurorozone II Rocket Program

Five Gerdien condensers--part of the XRG payloads--and two blunt probes measured middle atmosphere electrical parameters in the Aurorozone II program. Launch parameters for these rocket flights are listed in Table 4-2. For the XRG payloads, the outer return electrode and payload skin were grounded and the inner guard electrode and collector were biased at the sweep voltage (see Figure 3-2). With this probe biasing configuration, it can be shown that Equation (4-1) is still valid for reducing the electrical conductivity values.

The Gerdien condenser electrical conductivity data for the five XRG payload flights are presented chronologically in Figures 4-11 to 4-15.

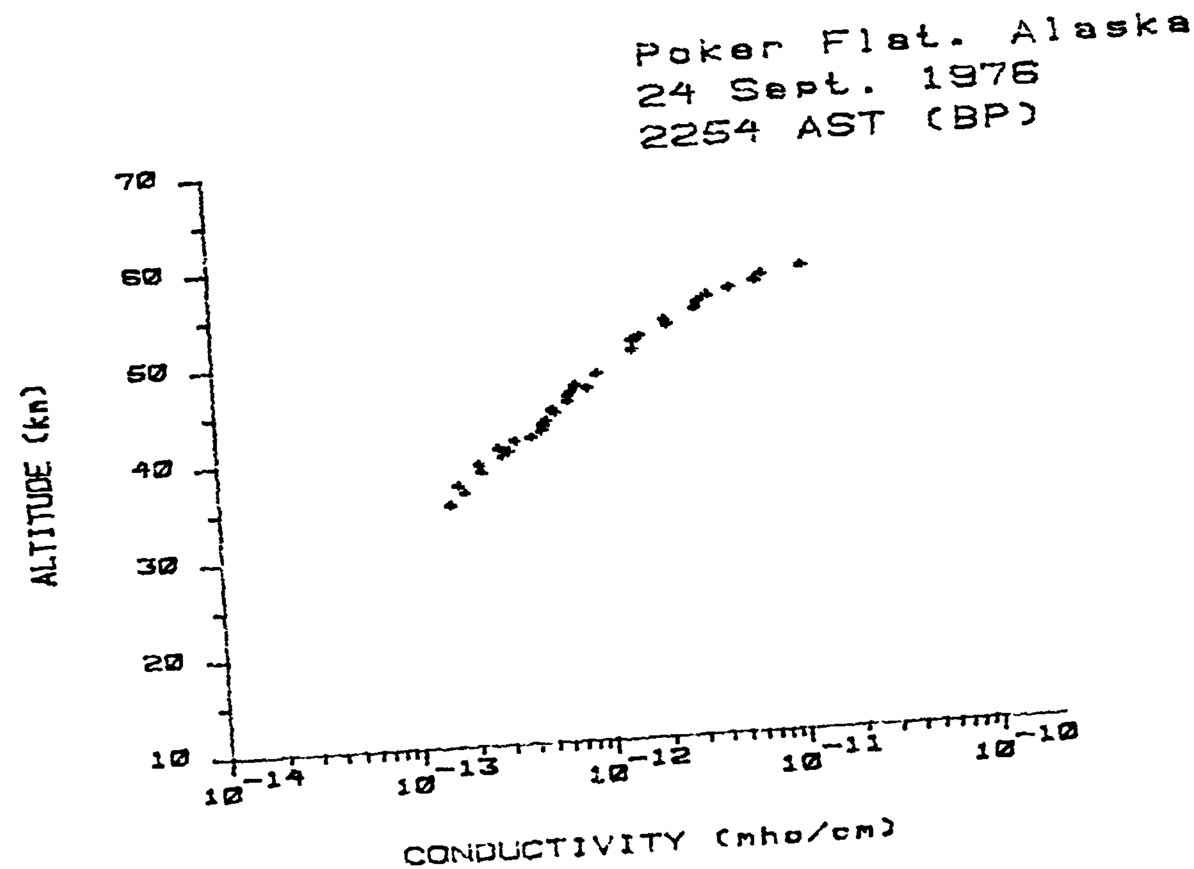

Figure 4-9. Positive Electrical Conductivity Measurements for 2254 AST on September 24, 1976

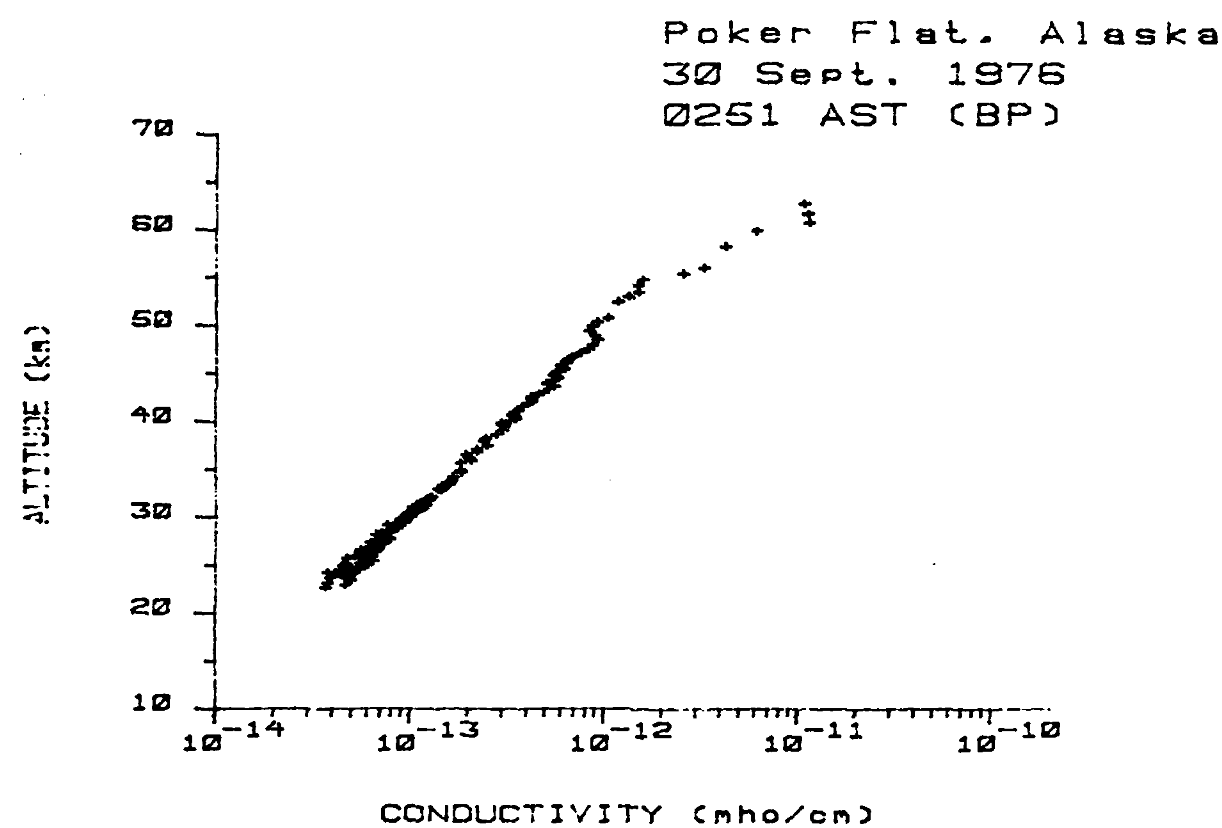

Figure 4-10. Positive Electrical Conductivity Measurements for 0251 AST on September 30, 1976

GERDIEN CONDENSER/BLUNT PROBE LAUNCH PARAMETERS FOR THE AURORОZONE II

ROCKET PROGRAM AT POKER FLAT, ALASKA (65°N, 173°W)

Launch Date (1978)	Launch Time (AST)	Instrument	Rocket	Geomagnetic Conditions
March 21	2052	Gerdien Condenser	Super Arcas	Quiet
March 21	2125	Blunt Probe	Super Loki	Quiet
March 27	0026	Gerdien Condenser	Super Arcas	Disturbed
March 29	0140:30	Gerdien Condenser	Super Arcas	Disturbed
March 29	0341:30	Blunt Probe	Super Loki	Disturbed
March 29	0649	Gerdien Condenser	Super Arcas	Disturbed
March 29	0740:30	Gerdien Condenser	Super Arcas	Disturbed
March 29	2045	Blunt Probe	Super Loki	Quiet

Table 4-2

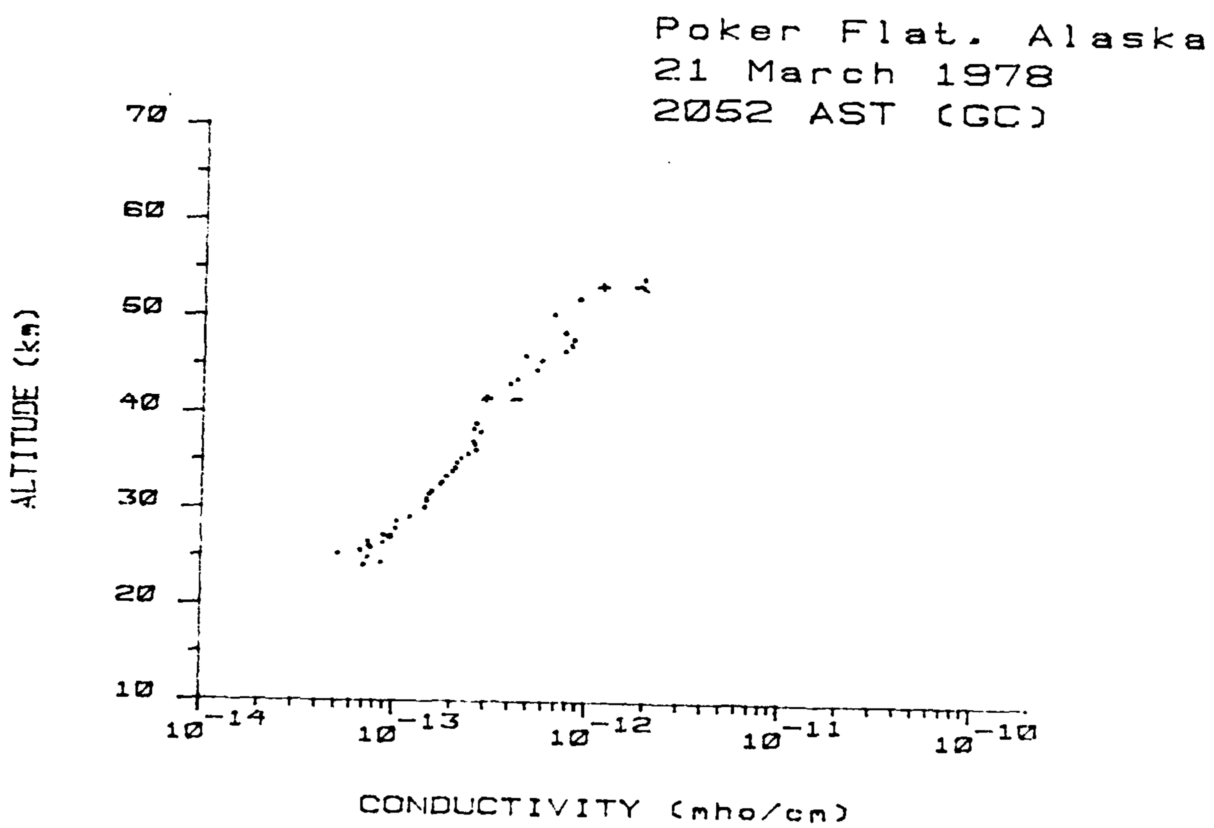

Figure 4-11. Electrical Conductivity Measurements for 2052 AST on March 21, 1978

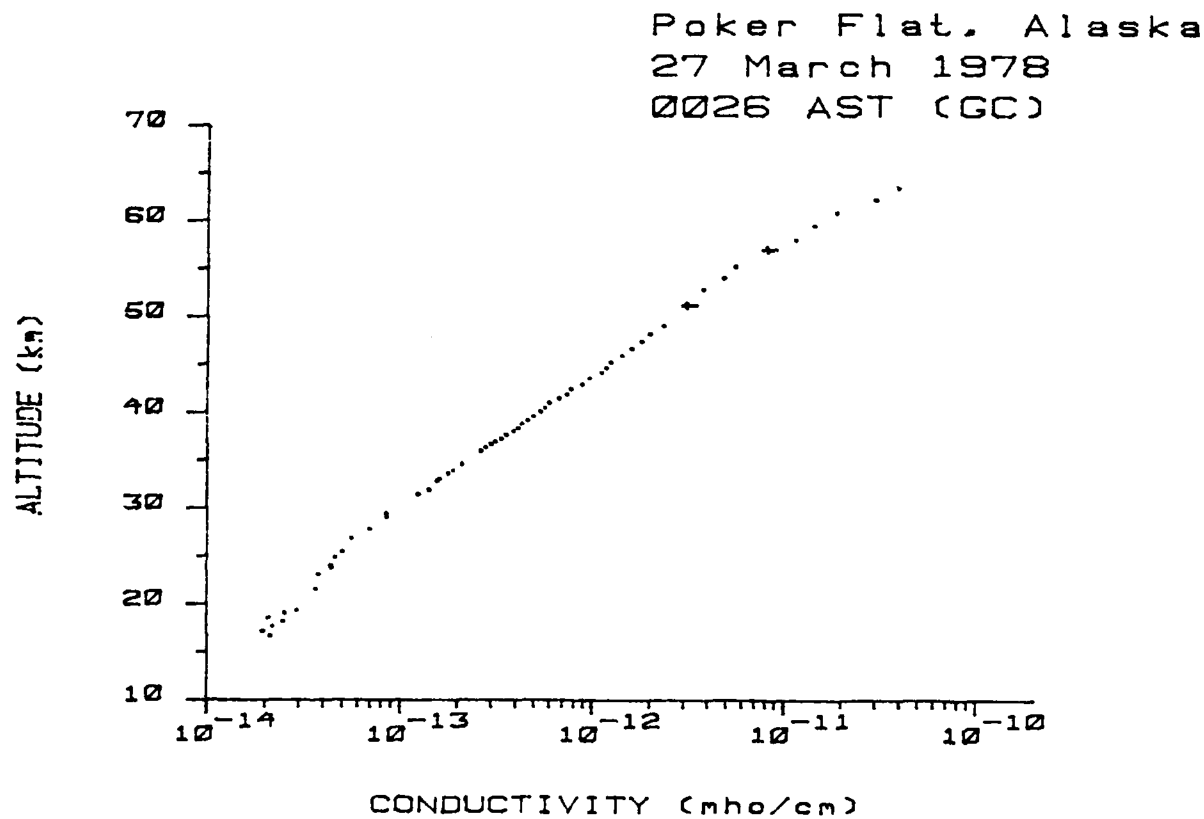

Figure 4-12. Electrical Conductivity Measurements for 0026 AST on March 27, 1978

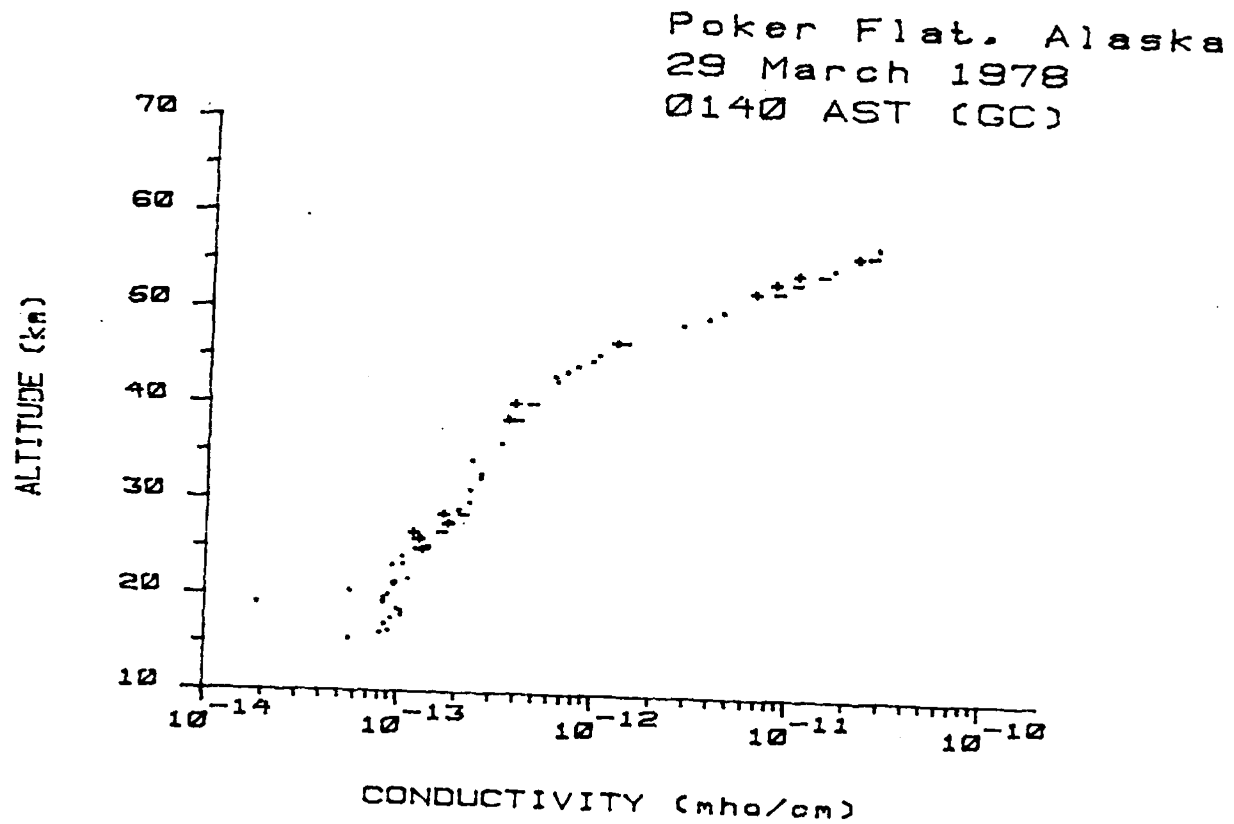

Figure 4-13. Electrical Conductivity Measurements for 0140 AST on March 29, 1978

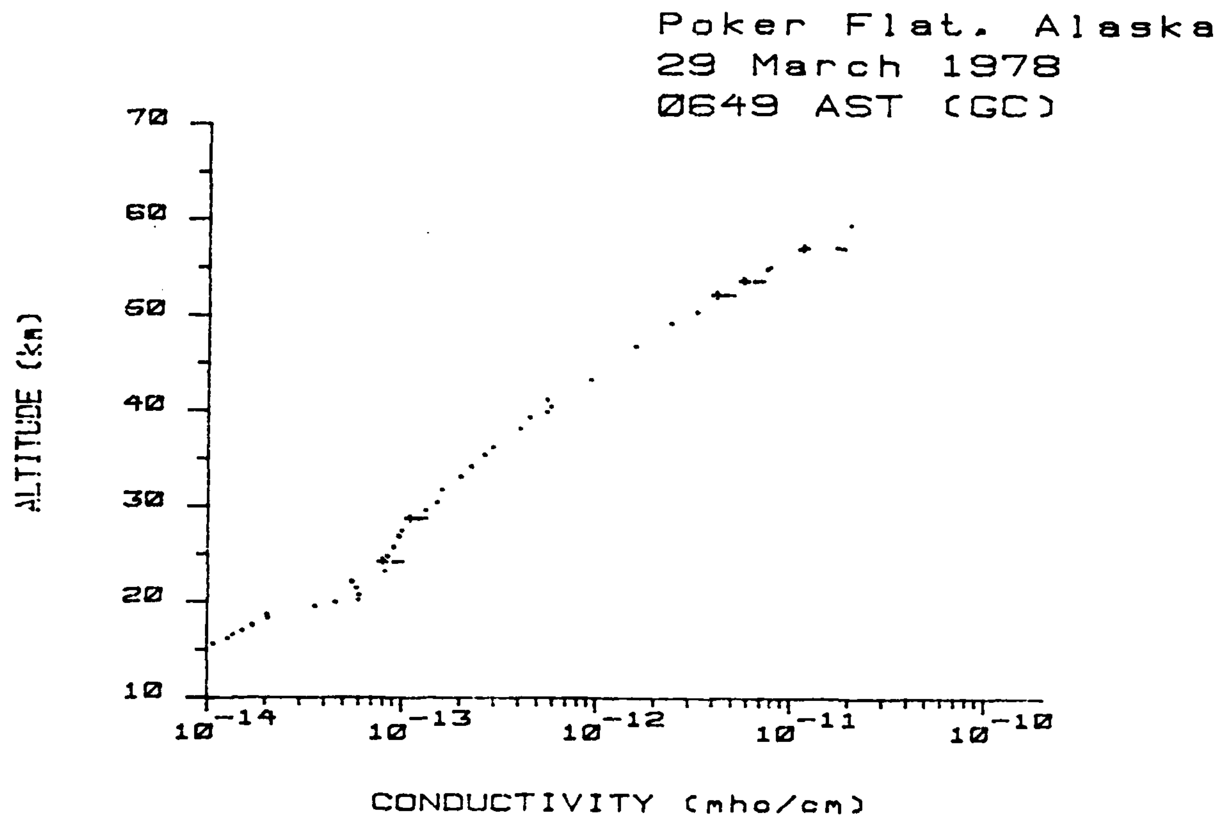

Figure 4-14. Electrical Conductivity Measurements for 0649 AST on March 29, 1978

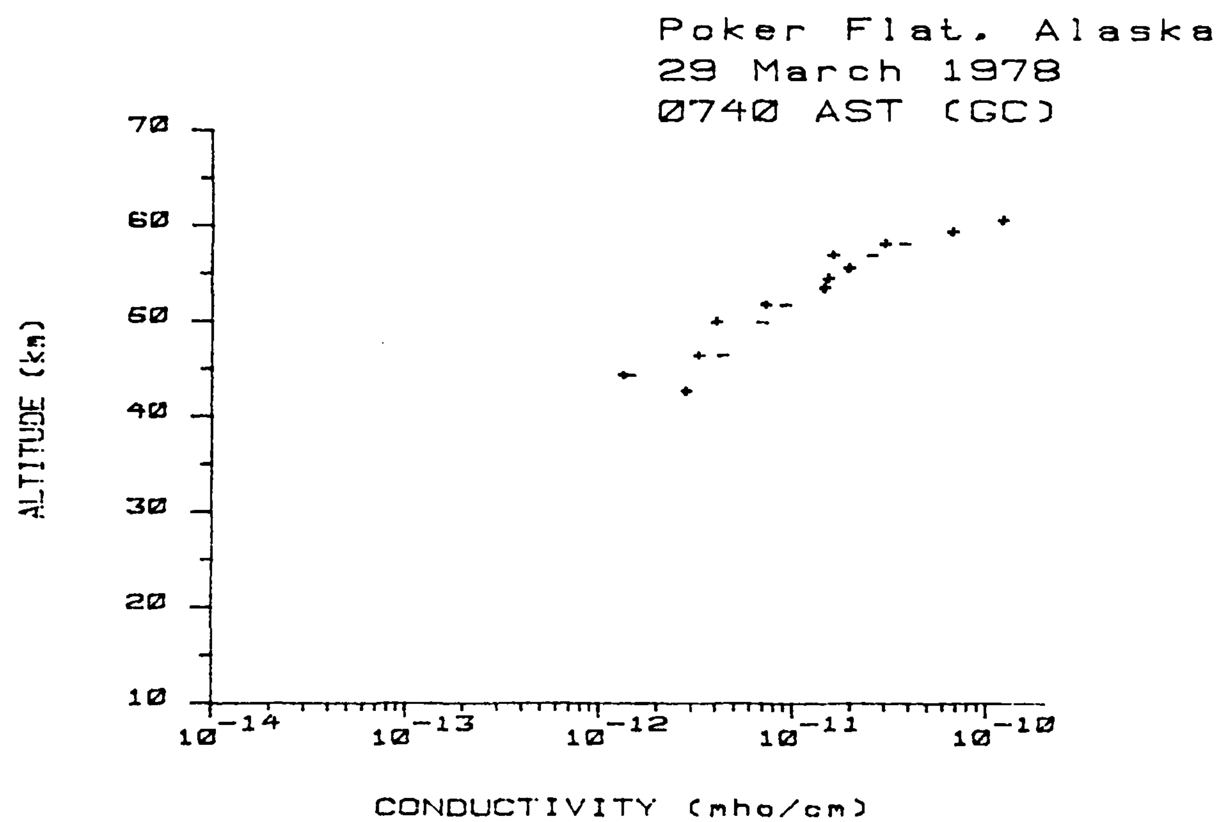

Figure 4-15. Electrical Conductivity Measurements for 0740 AST on March 29, 1978

CHAPTER V

DISCUSSION

The middle atmosphere electrical parameters measured by Gerdien condensers and blunt probes in the Aurorozone I and II rocket programs are discussed in this chapter. Geomagnetic conditions as determined from ground-based magnetometers and riometers at College Station and Fort Yukon, Alaska are qualitatively described for the launches in Tables 4-1 and 4-2. Although several flights in these tables are classified as occurring during geomagnetically quiet periods, probably the quietest period was the evening of March 21, 1978.

5.1 Aurorozone I Measurements

The Gerdien condenser and blunt probe rocket launches for the Aurorozone I program were all conducted at night since this period is usually more geomagnetically active. It also should be a somewhat simpler period for studying auroral ionization effects since there is no influence at higher altitudes from solar ionization sources.

Under geomagnetically quiet conditions, the dominant ionization source in the stratosphere and lower mesophere is associated with galactic cosmic rays, and it essentially displays an altitude dependence proportional to that for neutral number density. The corresponding altitude dependence for electical conductivity in the galactic cosmic ray ionization region is nicely demonstrated by the low altitude electrical conductivity data for the Aurorozone I program. As an example, the positive ion conductivity data for 2200 AST on September 22, 1976 are plotted in Figure 5-1, with a piecewise linear fit constructed to the data points. (Only positive ion conductivity data are shown for the Aurorozone I program. The negative conductivity measurements are generally comparable in value to the positive conductivity data.) The straight line fit at the lower altitudes is indicative of the altitude dependence of electrical conductivity in the galactic cosmic ray ionization region.

Above 50 km, the electrical conductivity values break to the right, indicating a conductivity enhancement above the associated galactic cosmic ray background level (shown by the dashed line). Interestingly, it is also possible to construct a straight line fit to these high altitude data. The enhancement in conductivity is thought to result from aurorally-induced bremsstrahlung X-ray ionization. The breakpoint for the piecewise linear fit to the data thus shows how low the bremsstrahlung X-ray ionization penetrates into the atmosphere.

The presence of this additional ionization source at higher altitudes is substantiated by the X-ray data obtained from the two Nike-Tomahawk flights (September 21 and 23, 1976). Energy deposition deduced from the X-ray energy data for

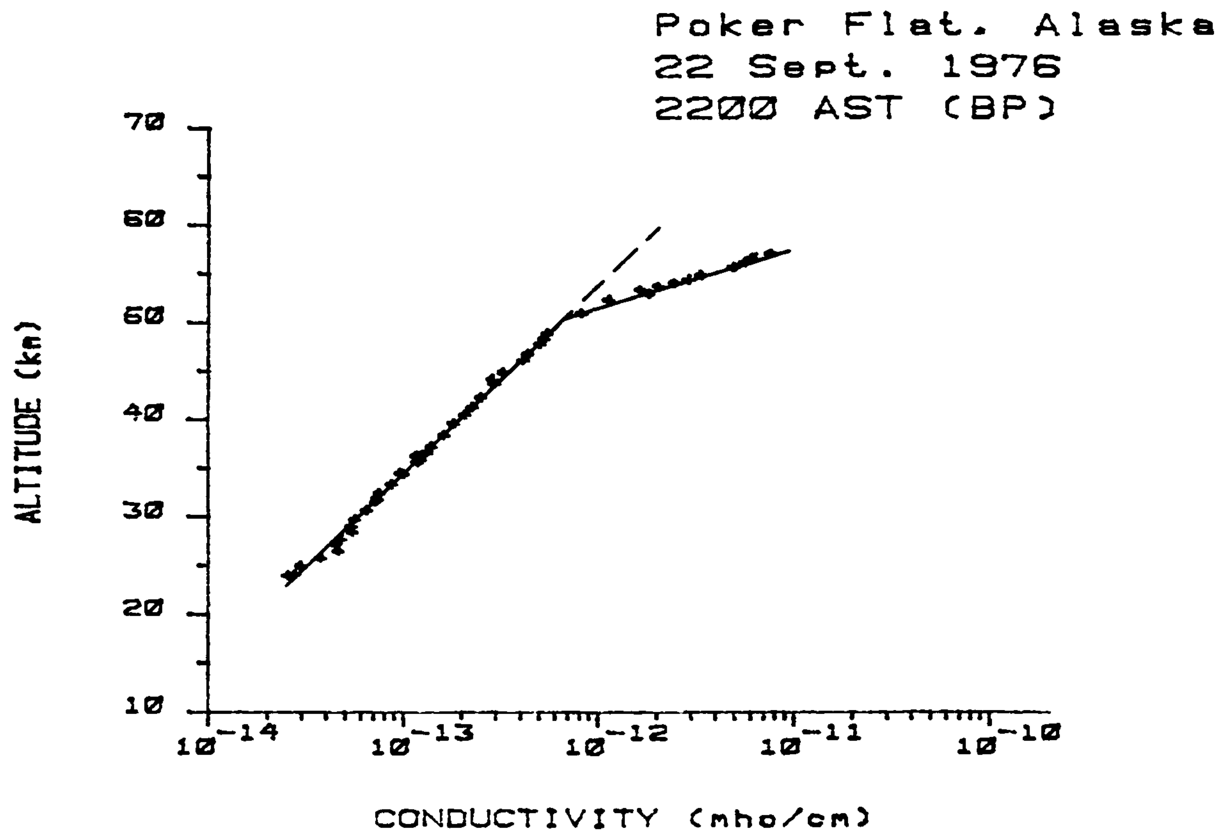

Figure 5-1. Piecewise Linear Fit to the Positive Conductivity Measurements for 2200 AST on September 22, 1976

September 23 are shown in Figure 5-2 [Goldberg and Hilsenrath (1978)]. Examining this figure, we see that the energy deposited below approximately 40 km is primarily from galactic cosmic rays. In the 40 to 55 km altitude region, ionization is largely associated with 5 keV bremsstrahlung X-rays. At higher altitudes, 100 keV energetic particles become an important ionization source.

The general altitude structure for the September 22, 1976 conductivity data is actually observed to some extent in all of the Aurorozone I measurements. A composite of the piecewise linear fits constructed for five sets of positive conductivity data from the Aurorozone I program is shown in Figure 5-3. The legend in the figure identifies the different curves and also indicates the corresponding altitudes of the ionization breakpoints.

For the night of September 22 to 23, 1976 which was the most active of the measurement period, the bremsstrahlung X-ray ionization effects are observed as low as 45 km (following an auroral event). In fact, the three sets of data obtained during that night show the X-ray ionization effects penetrating continually lower as the event progresses. The data for September 21, 1976 were also obtained during a period of geomagnetic activity. The activity for this period was not as strong, as might be inferred from the relatively higher ionization breakpoint (approximately 51 km).

The electrical conductivity data for 0251 AST on

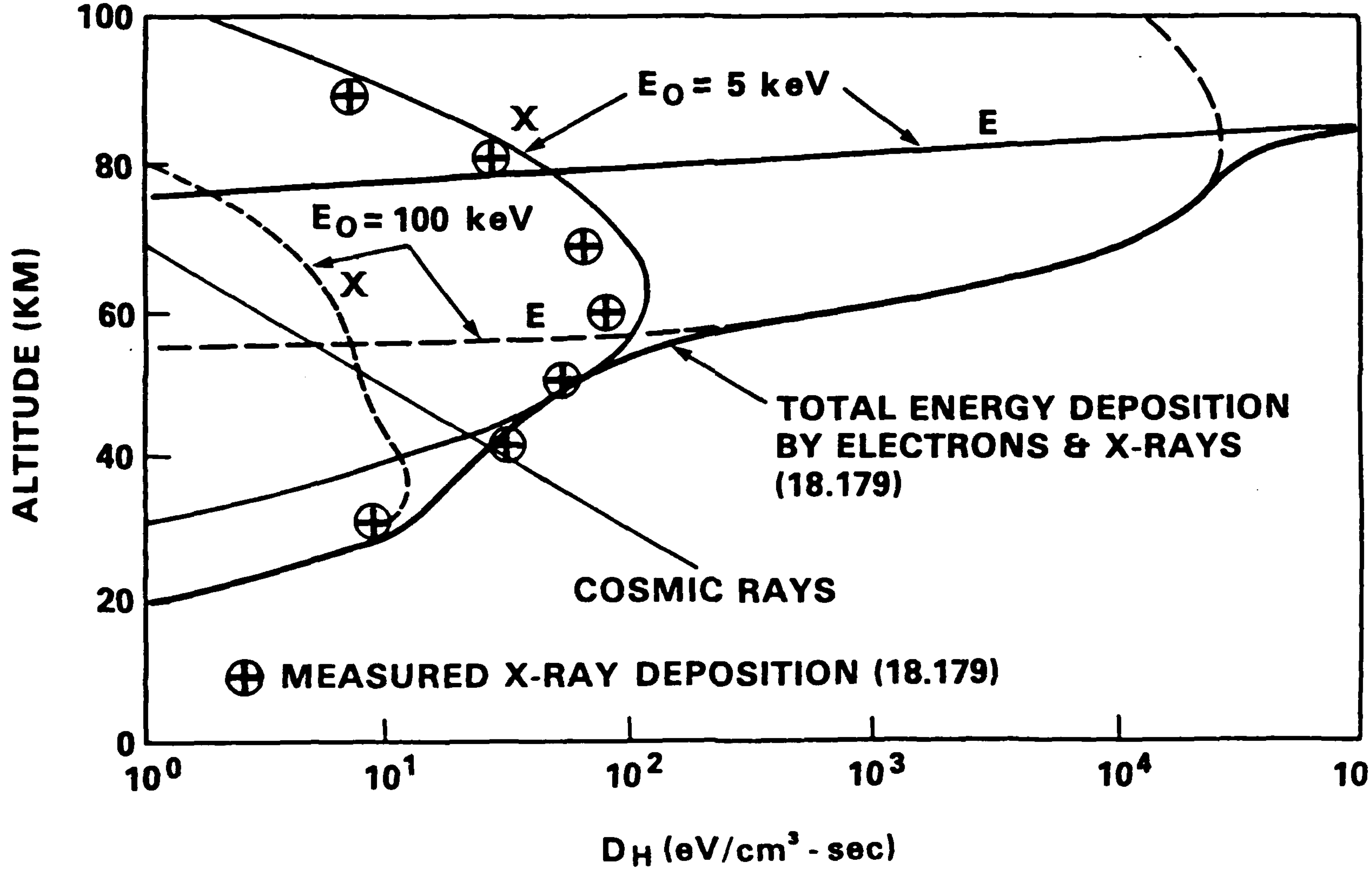

Figure 5-2. Total Energy Deposition for 0137 AST on September 23, 1976

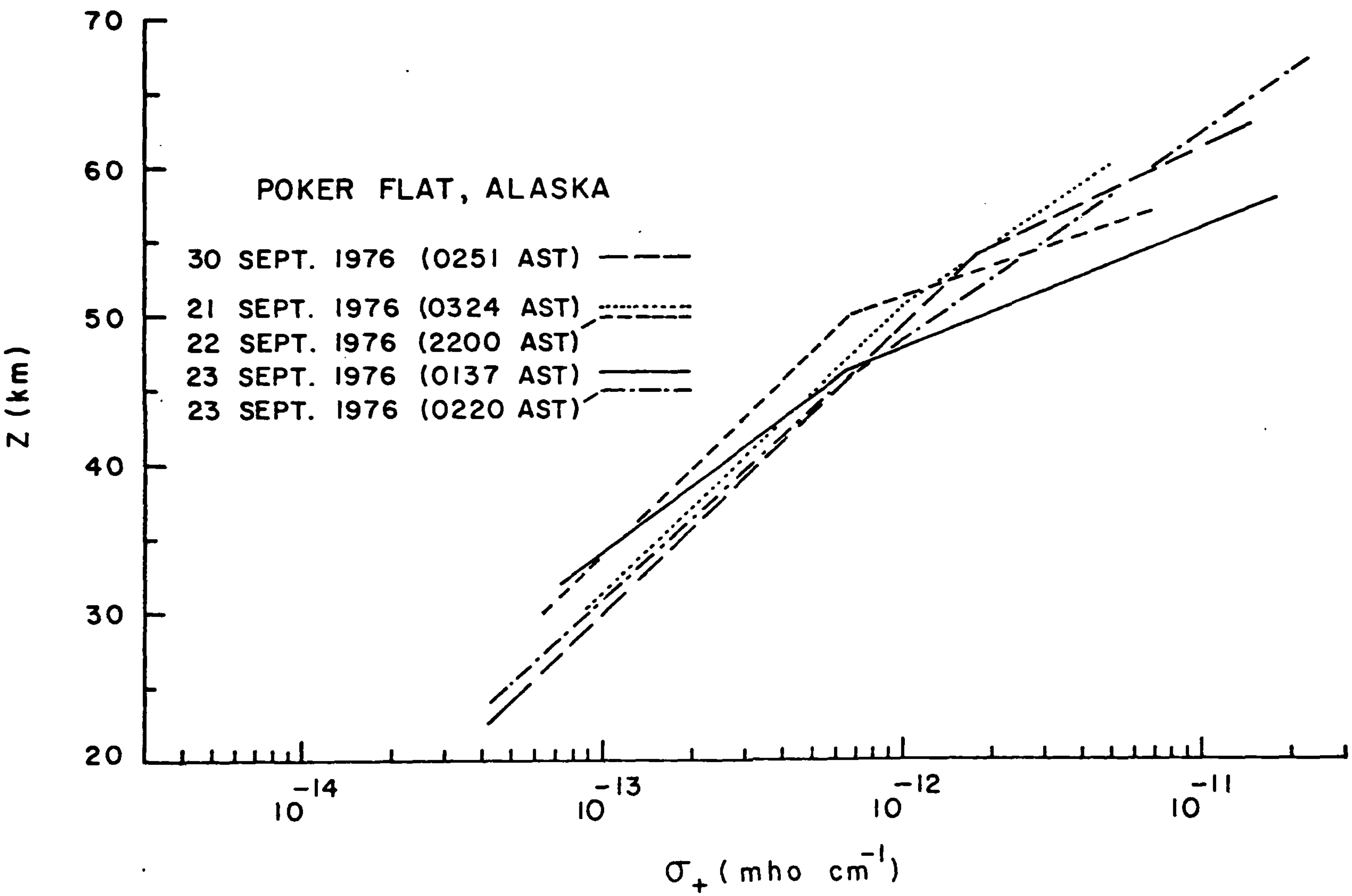

Figure 5-3. Composite of Piecewise Linear Fits to the Positive Conductivity Measurements for the Aurorozone I Program

September 30, 1976 were obtained during the quietest measurement period of the Aurorozone I program. Based on the conductivity enhancements observed above 54 km, it would appear that this period was not actually that quiet. In fact, there were probably ionization effects due to auroral energetics present to some extent throughout the entire measurement period.

Conductivity measurements for the three-launch sequence on the night of September 22 to 23, 1976 are shown in Figure 5-4. With the data for 2200 AST used as the reference, we see conductivity enhancements in the high altitude data for 0137 AST which was the most active period during the auroral event. The positive conductivity data obtained at 0220 AST following the event, however, show a recovery from the conductivity build-up at higher altitudes. Interestingly, at the lower altitudes where it appears the bremsstrahlung X-rays do not penetrate, an overall increase in ion conductivity is observed.

As developed earlier, the Gerdien condenser measures ion mobility and charge number density as well as electrical conductivity. The ion mobility and charge number density values for 0220 AST on September 23, 1976 are shown in Figure 4-7 and 4-8, respectively. As many as three distinct positive ion mobility groups were measured at some of the higher altitudes. In general, it appeared that ion saturation was not achieved which would imply that at least one

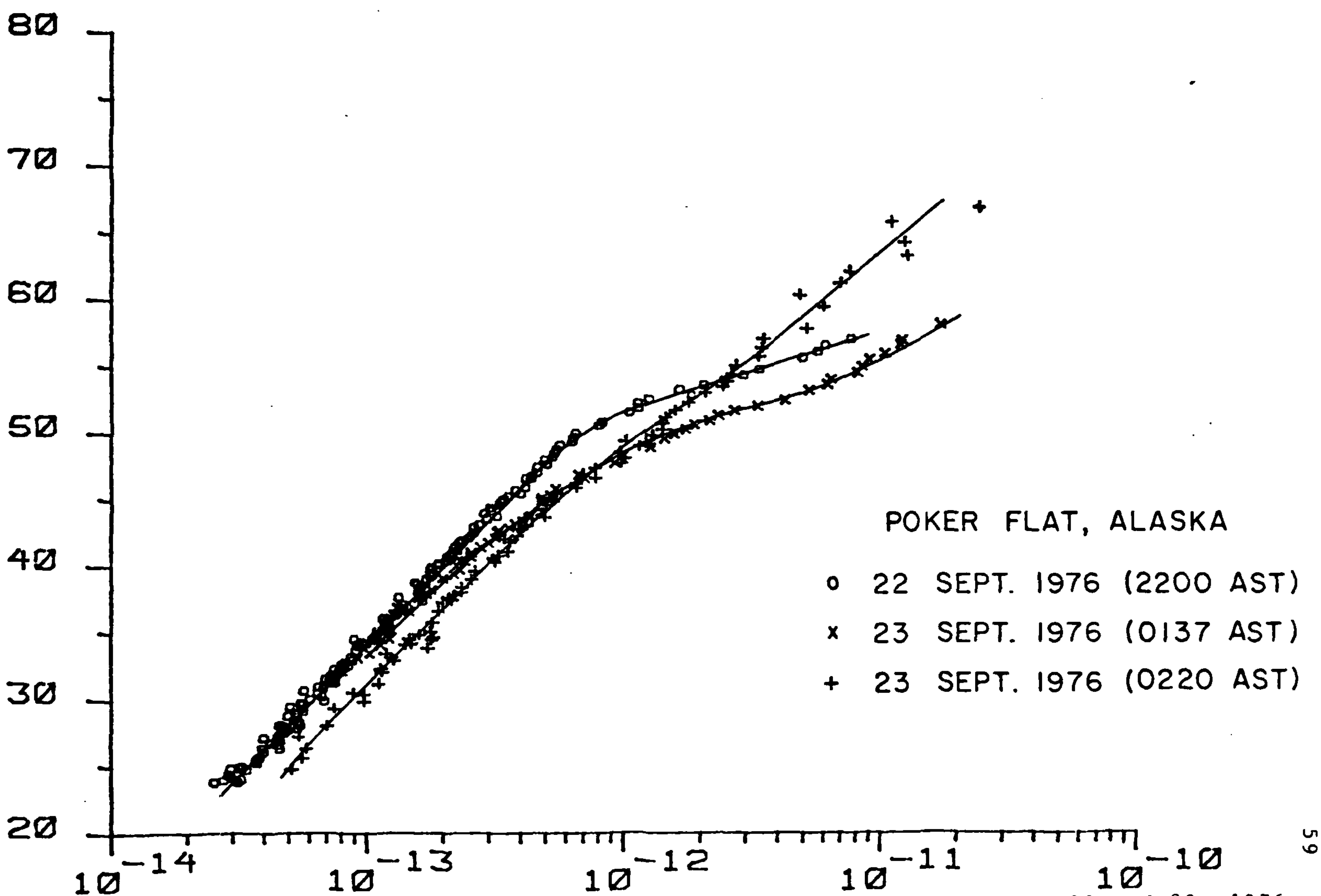

Figure 5-4. Positive Electrical Conductivity Measurements on September 22 and 23, 1976

additional mobility group with values to the left of the dashed line was also present in the air sample. The straight line in Figure 4-7 is drawn to fit the highest mobility group, which is present over the entire altitude region.

The positive ion concentrations corresponding to the different ion mobility groups in Figure 4-7 are shown in Figure 4-8. The highest ion mobility group has a concentration of approximately 10^3 cm^{-3} over the entire altitude region, with the less mobile ions having generally smaller number densities.

If the ion mobility values (Figure 4-7) for the highest mobility group and the corresponding number density values (Figure 4-8) are used to compute electrical conductivity, it is observed that this particular mobility group accounts for the electrical conductivity component associated with galactic cosmic ray ionization. The less mobile groups, which are observed at the higher altitudes where there is ionization by bremsstrahlung X-rays, appear to account for the enhancement in conductivity above the galactic cosmic ray ionization level. Possibly, the less mobile ion species result directly from this additional ionization source, but more likely, the bremsstrahlung X-rays influence the chemical processes in the region leading to the formation of less mobile species.

Similar results are observed for the Gerdien condenser ion mobility (Figure 4-2) and charge number density (Figure 4-3) data for 0324 AST on September 21, 1976. It should be noted that both Gerdien condenser rocket flights for the Aurorozone I rocket program occurred during geomagnetically disturbed conditions and thus no ion mobility and charge number density data were obtained for quiet conditions. As mentioned earlier, even the electrical conductivity data obtained during periods which appeared from ground-based measurements to be geomagnetically quiet were, in fact, also affected by auroral energetics.

5.2 Aurorozone II Measurements

The XRG payloads flown in the Aurorozone II program were heavier than the Gerdien condensers in the Aurorozone I program, and thus measurements above 60 km are limited. Futhermore, the Gerdien condenser launch schedule for the Aurorozone II program is more diversified, including night-time launches under both geomagnetically quiet (2052 AST on March 21, 1978) and disturbed (0026 AST on March 27 and 0140 AST on March 29, 1978) conditions and launches during morning twilight under geomagnetically disturbed conditions (0649 AST and 0740 AST on March 29, 1978). The dots in Figures 4-11 to 4-15 represent measurements for which the positive and negative conductivity values are equal. The plus and minus signs include instances when there were small differences in the respective positive and negative conductivity measurements. In general, we see that the differences in the polar conductivity values at these altitudes are relatively small.

The electrical conductivity measurements for March 21, 1978 (Figure 4-11) are in general agreement with what is expected for geomagnetically quiet conditions. The altitude dependence for electrical conductivity throughout the entire measurement region would indicate that galactic cosmic ray ionization is the dominant source for ions, and no noticed ionization enhancements associated with auroral energetics appear significant at the higher altitudes. A wave-like effect on the conductivity data is observed at the higher altitudes which possibly reflects the dependence of ion mobility on pressure. Considerable payload swing was observed during the flight making further reduction of the data to determine ion mobility and charge number density a difficult task.

The two nighttime conductivity measurements obtained under geomagnetically disturbed conditions in the Aurorozone II program demonstrate general trends consistent with the data for the Aurorozone I program. If the electrical conductivity measurements for March 21, 1978 (Figure 4-11) are used as a reference, the data for March 27, 1978 (Figure 4-12) show enhancements in electrical conductivity at all altitudes above 37 km. The nighttime electrical conductivity measurements for March 29, 1978 (Figure 4-13) are relatively larger than the reference values for March 21, 1978 at all altitudes.

Probably the most interesting result is observed in comparing the three sets of nighttime data at the lower altitudes. While there is generally good agreement between the data sets for March 21 and 27, 1978, which is to be expected if the ionization is principally controlled by galactic cosmic rays, the nighttime measurements for March 29, 1978 show a marked enhancement in conductivity. Thus, it would appear that the auroral energetics do, on occasion, influence ionization processes even in the lower stratosphere.

The morning twilight data for 0649 AST and 0740 AST on March 29, 1978 (Figures 4-14 and 4-15, respectively) were obtained during a geomagnetically disturbed period. The battery life was relatively short for the payload flown at 0740 AST, and thus electrical conductivity data were obtained only down to 43 km. If the electrical conductivity measurements for either of these flights are compared to the reference data of March 21, 1978 obtained under geomagnetically quiet conditions, there are observed conductivity enhancements at higher altitudes which are again thought to be associated with auroral energetics.

In comparing the two morning twilight conductivity measurements, it is observed that the conductivity values for 0740 AST are relatively larger than these for 0649 AST.

This early morning enhancement in conductivity at these altitudes is thought to be at least partly attributed to a photodissociation process resulting in the formation of more mobile ion species [Mitchell, Sagar and Olsen (1977)].

CHAPTER VI

CONCLUSIONS

6.1 Summary

The initial results from high-latitude ionization studies of the middle atmosphere indicate that auroral energetics strongly influence electrical parameters in this altitude region. Nighttime measurements of electrical conductivity from two field programs at Poker Flat, Alaska —— Aurorozone I and II —— showed enhancements in electrical conductivity during periods of auroral activity. These conductivity enhancements in the stratosphere are thought to result from ionization by bremmstrahlung X-rays emitted at higher altitudes. The region in which the conductivity enhancements were observed corresponds to the altitudes in which X-rays were measured by other experiments flown in these programs.

The Gerdien condensers were also used to measure ion mobility and charge number density in addition to electrical conductivity. The ion mobility data from the two Gerdien condenser flights in the Aurorozone I program indicate the presence of additional lower-valued ion mobility groups in the region where the bremmstrahlung X-ray ionization is observed. Furthermore, the conductivity values computed using these particular mobility groups and their corresponding density values account for the bremmstrahlung X-ray-associated conductivity enhancements. Thus, it appears that the ion chemistry is modified by the auroral energetics, resulting in the formation of new and different ion species.

6.2 Suggestions for Future Research

Further studies are needed to better understand how middle atmosphere electrical parameters and other neutral parameters are affected by auroral energetics. Such programs preferrably should include integrated instrument packages such as the XRG payload which is capable of measuring both the source parameters and the affected electrical parameters. Finally, a complete understanding of auroral related energetics and their influence on ion chemistry also requires that measurements be made during geomagnetically quiet conditions.

REFERENCES

1. Aikin, A.C., Ionization sources of the ionospheric D and E regions, Aeronomy Report No. 48, 96, 1972.

2. Berger, M.J., S.M. Seltzer and K. Maeda, Some new results on electron transport in the atmosphere, J. Atmos. Terr. Phys. 36, 591, 1974.

3. Conley, T.D., Mesospheric positive ion concentration mobility and loss rates obtained from rocket-borne Gerdien condenser measurements, Radio Sci. 9, 575, 1974.

4. Croskey, C., In situ measurements of the mesosphere and stratosphere, Scientific Report No. 442, Ionosphere Research Laboratory, Pennsylvania State University (1976).

5. Farrokh, H., Design of a simple Gerdien condenser for ionospheric D-region charged particle density and mobility measurements, Scientific Report No. 433, Ionosphere Research Laboratory, Pennsylvania State University (1975).

6. Freyer, G.J., Bremsstrahlung in the lower ionosphere, Scientific Report No. 336, Ionosphere Research Laboratory, Pennsylvania State University (1969).

7. Goldberg, R.A. and E.R. Hilsenrath, Operation Aurorozone: An experiment in Sun/Weather in third NASA weather and climate program science review, ed. by E.R. Kreins, NASA CP 2029, 121, 1978.

8. Hale, L.C., Parameters of the low ionosphere at night deduced from parachute borne blunt probe measurements, Space Res. VII, 140, 1967.

9. Hale, L.C., D.P. Hoult and D.C. Baker, A summary of blunt probe theory and experimental results, Space Res. VII, 320, 1968.

10. Mitchell, J.D., An experimental investigation of mesospheric ionization, Scientific Report No. 416, Ionosphere Research Laboratory, Pennsylvania State University (1973)

11. Mitchell, J.D., R.S. Sagar and R.O. Olsen, Positive ions in the middle atmosphere during sunrise conditions, Space Research XVII, 199, 1977.

REFERENCES (cont'd)

12. Pedersen, A., Measurement of ion concentration in the D-region of the ionosphere with a Gerdien condenser rocket probe, FOA 3 Report A607, Research Institute of National Defense, Stockhom, Sweden (1964).

13. Pomerantz, M.A. and S.P. Duggal, The sun and cosmic rays, Rev. Geophys. Space Phys., 12, 343, 1974.

14. Rose, G. and H.U. Widdel, Results of concentration and mobility measurements for positively and negatively charged particles taken between 85 and 22 km in sounding rocket experiments, Radio Sci.77, 81, 1972.

15. Sagar, R.S., A subsonic Gerdien condenser experiment for upper atmospheric research, Thesis Department of Electrical Engineering, University of Texas at El Paso (1976).

16. Velinov, P., On ionization in the ionospheric D-region by galactic cosmic rays, J. Atmos. Terr. Phys. 30, 1891, 1968.

17. Webber, W.R., The production of free electrons in the ionospheric D layer by solar and galactic cosmic rays and the resultant absorption of radio waves, J. Geophys. Res. 67, 5091, 1962.